INVESTIGATIONS ON MULTIBAND BEHAVIOR OF MICROSTRIP ANTENNAS

By

WITHEYA SUWANNO A/L PET

FINAL PROJECT REPORT

Submitted to the Electrical & Electronics Engineering Programme
in Partial Fulfillment of the Requirements
for the Degree
Bachelor of Engineering (Hons)
(Electrical & Electronics Engineering)

Universiti Teknologi Petronas
Bandar Seri Iskandar
31750 Tronoh
Perak Darul Ridzuan

CERTIFICATION OF APPROVAL

INVESTIGATIONS ON MULTIBAND BEHAVIOR OF MICROSTRIP ANTENNAS

by

Witheya Suwanno A/L Pet

A project dissertation submitted to the
Electrical & Electronics Engineering Programme
Universiti Teknologi PETRONAS
in partial fulfilment of the requirement for the
Bachelor of Engineering (Hons)
(Electrical & Electronics Engineering)

Approved:

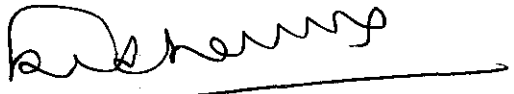

Professor Dr. P. C. Sharma

Project Supervisor

UNIVERSITI TEKNOLOGI PETRONAS
TRONOH, PERAK

June 2004

CERTIFICATION OF ORIGINALITY

This is to certify that I am responsible for the work submitted in this project, that the original work is my own except as specified in the references and acknowledgements, and that the original work contained herein have not been undertaken or done by unspecified sources or persons.

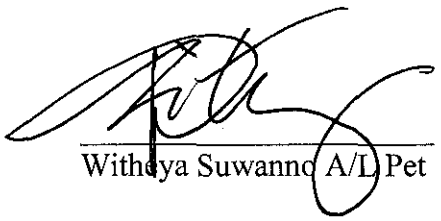

Withaya Suwanno A/L Pet

ABSTRACT

Microstrip antennas have become popular in the advent of cellular communication technology due to their compact size, light weight, ease of fabrication, reliability, and thin profile that makes their mounting conformal. If a single antenna can be used for multi frequency operation, the complexity of the mobile communication antenna system could be reduced.

Exploiting the frequency reuse and smart antenna characteristics could result in cost reduction and enhancing the communication quality and range. The foreseen potential of these aspects ought to be further explored and studied for future benefits and hence, has led to the proposal of this project entitled "Investigation on Multiband Behavior of Microstrip Antenna".

The objectives of the project are to familiarize with the concepts of microstrip antenna and to analyze the multiband behavior of microstrip antenna in terms of the multiband characteristics, frequency separation of bands, resonant frequency dependency on dimensions and slot positions, and the effect of feed location on the antenna behavior.

The project work would analyze typical rectangular microstrip antenna structures by modeling and simulating the antenna structure using HP High Frequency Structure Simulator (HP HFSS) software and to conclude on the findings.

ACKNOWLEDGEMENT

The present project work was carried out from August 2003 to May 2004 under the supervision of Professor Dr. P. C. Sharma, co-supervized by Associate Professor Dr. Varun Jeoti and Mr. Zainal Arif Burhanuddin from Electrical and Electronics Engineering Program of Universiti Teknologi Petronas. The author would like to acknowledge his supervisors for providing the valuable guidance and advice needed to complete this project.

The author wishes to record his thanks to his project partners, Ang Ai Leen and Salisa Abdul Rahman, who had work along with him for their support and cooperation during the duration of the project.

Last but not least, the author's gratitude to Mr. Gobi Vetharatnam from Multimedia University who shared his experience in using simulation software for high frequency circuit.

TABLE OF CONTENTS

LIST OF FIGURES

LIST OF TABLES

CHAPTER 1

INTRODUCTION

1 INTRODUCTION

The project, "Investigation on Multiband Behavior of Microstrip Antennas" requires an analysis on the electromagnetic behavior and characteristics of microstrip antenna. Various aspects will be studied in order to investigate the multiband characteristics of this antenna, which will be further discussed in this report.

1.1 Background

The increase in the number of mobile communication devices and satellite communications has meant an increase in the need for antennas that integrate into ever-smaller devices. Microstrip antennas have, in recent years, become quite useful due to their compact size, light weight, thin profile that makes their mounting conformal, ease of fabrication, reliability and the multiband behavior.

1.2 Problem Statement

The development and advancement of mobile communication demands for multiband antenna systems. The complexity of the antenna system required in mobile communication would be reduced if a single antenna can be used for multi-frequency operation. If the frequency reuse and smart antenna characteristics are exploited fully, it may render communication services at reduced cost and at the same time enhancing the quality and range of communication. With this aspect in mind, an investigation on microstrip antennas for their multi-frequency operation was proposed.

1.3 Objectives

The project attempts to address the following objectives:

- To simulate and analyze typical rectangular microstrip antenna for multiband behavior.
- To analyze the multiband characteristics and frequency separation of bands.
- To analyze the dependence of frequencies of resonance for various bands on dimensions and slot positions.
- To analyze the effect of feed location on the antenna behavior.

1.4 Scope of Study

This research based project provides opportunity for the author to become familiar with the concept of microstrip antenna, their characterization as well as the usage of software for simulation and studies of high frequency circuits. The project work will include the task of analyzing some microstrip antenna structures using HP High-Frequency Structure Simulator, HP HFSS software.

The work basically includes simulation of rectangular antenna structure and exploring the multiband behavior of this antenna from the point of view of feed port location, bandwidth and separation of frequencies. Analysis need to be done on the multiband characteristic, frequency separation of bands, dependency of resonance frequencies for various bands on dimensions and slot positions, and also the effect of feed location on the antenna behavior.

At the end, the author needs to summarize the results and provide the concluding remarks on the work done. The project is concluded feasible to be conducted in the given timeframe and within the scope defined.

CHAPTER 2

LITERATURE REVIEW AND THEORY

2 LITERATURE REVIEW AND THEORY

From the literature review, the major interest would be understanding the basics of microstrip antenna which serve as an introduction to microstrip antenna. The configuration, characteristics, theory and concepts of microstrip antenna are prerequisite knowledge in pursuing with this project. The related information such as boundary condition, fractals and the transmission line characteristics are important in order to gain an insight view of the project.

2.1 Microstrip Antenna Configuration and Characteristics

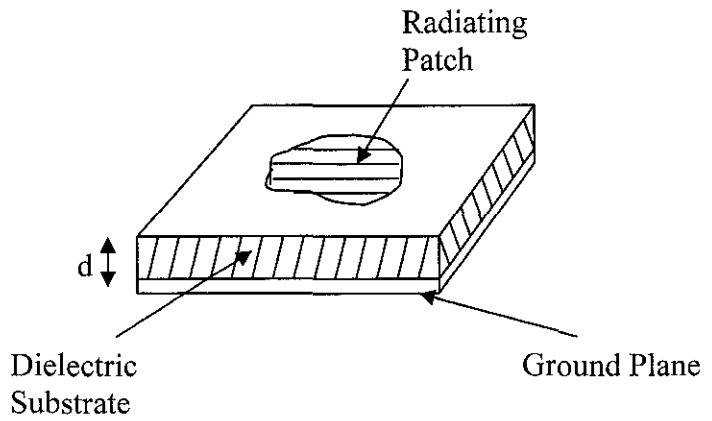

Figure 2-1: Simplified microstrip antenna configuration

Microstrip is simply a flat conductor separated from ground by an insulating dielectric material. An antenna is a metallic conductor system capable of radiating and capturing electromagnetic waves. Antennas are used to interface transmission lines to free space, free space to transmission lines, or both [1]. The simplest configuration of

microstrip antenna consists of a radiating patch on one side of a dielectric substrate which has a ground plane on the other side. The dielectric constants of the substrate are usually in the range of $2.2 \leq \epsilon_r \leq 12$. The thickness of the substrate, d, is usually very small compared to the wavelength ($d<<\lambda$). The patch, usually of copper or gold can be of any shape. Square, rectangular, dipole, and circular are widely used due to ease of analysis, fabrication and low cross-polarization radiation [2], [3].

2.2 Feeding Methods

There are various ways in which a microstrip antenna can be fed. Four most popular configurations are the microstrip line, coaxial probe, aperture coupling and proximity coupling.

2.2.1 Microstrip Line

The microstrip feed line is also a conducting strip of much smaller width in comparison to the patch. The microstrip feed line is easy to fabricate, can be matched by controlling the inset position and not difficult to model. However, the surface waves and spurious feed radiation will increase as the substrate thickness increases and this could lead to limitation on bandwidth. The rectangular microstrip antennas studied in this project would be using microstrip line feed.

2.2.2 Coaxial-Line

For this configuration, the inner conductor of the coax is attached to the radiation patch while the outer conductor is connected to the ground plane. Coaxial probe feed is also easy to fabricate and match but it has a low spurious radiation. However, it is difficult to model and has narrow bandwidth.

2.2.3 Aperture Coupling

Aperture coupling consists of two substrates separated by a ground plane. There is a microstrip feed line on the bottom side of the lower substrate whose energy is coupled to the patch through a slot on the ground plane separating two substrates This configuration is the most difficult among the four to be fabricated and it has narrow bandwidth. But it is easier to model and has moderate spurious radiation.

2.2.4 Proximity Coupling

Proximity coupling consists of a microstrip line placed between two substrates. It has the largest bandwidth among the four, easy to model and has low spurious radiation. However it is more difficult to be fabricated.

2.3 Boundaries Overview

Any plane, object surface, or interface between two objects may be defined as a boundary and assigned a boundary condition. This section briefly describes the kinds of boundaries that can be modeled in HP HFSS.

2.3.1 Port

A port is a type of boundary condition that permits energy to flow into and out of an area of a structure. By default, a structure is assumed to be completely encased in a conductive shield with no energy propagating to or from the background. Ports represent locations in the geometry through which waves may propagate into or out of a structure.

2.3.2 Perfect H

Perfect H is a perfect magnetic boundary. This type of boundary forces the magnetic field (H-field) to be normal to a surface.

2.3.3 Perfect E

Perfect E is a perfect electric boundary, also referred to as a perfect conductor. This type of boundary forces the electric field (E-field) to be normal to the surface.

2.3.4 Symmetry Planes

A plane of symmetry exists whenever a structure has geometric and electromagnetic symmetry – that is, the fields in one half of the structure are either identical to or are the mirror image of the fields in the other half of the structure. Symmetry planes can be treated like other structure surfaces and assigned boundary conditions. Taking advantage of symmetry planes can simplify simulations and reduce simulation run times.

2.3.5 Ground Plane

Generally, the ground plane is treated as an infinite, Perfect E boundary condition. If radiation boundaries are used in a structure, the ground plane acts as a shield for far-field energy, preventing waves from propagating past the ground plane.

2.3.6 Conductor

A conductor boundary enables definition of a surface of an object as a lossy conductor. It is an imperfect E boundary condition, and is analogous to the lossy metal material definition. To model a surface as lossy, Siemens/meter and permeability parameters enable a surface that is an imperfect conductor to be specified. Loss is calculated as a function of frequency.

2.3.7 Resistor

A surface or boundary can be modeled as impedance and the real and imaginary parts of an impedance can be described in ohms/square. The resistivity is constant and does not change with frequency.

2.3.8 Radiation Boundary

Radiation boundaries, also referred to as absorbing boundaries, enable a surface to be modeled as open: waves radiate outward, infinitely far into space. The system absorbs the wave at the radiation boundary, essentially ballooning the boundary infinitely far away from the structure. Radiation boundaries may also be placed relatively close to a structure and can be arbitrarily shaped. This condition eliminates the need for a spherical boundary. For structures that include radiation boundaries, calculated S-parameters include the effects of radiation loss.

2.3.9 Restore

The restore boundary condition reverts the selected area to its original material, erasing any imposed boundary condition. This can be used, for example, to model a horn antenna opening inside of a radiation boundary.

2.3.10 Sources

Sources are used to inject energy into a structure as an alternative to ports. A source can be assigned to any 2D object, 3D object surface, or boundary. The source output (volts, amperes, or watts) must be defined when the results are displayed.

2.4 Fractals and Multiband Behavior of Antenna

Discovered by Mandelbrot in the 1970s, fractal is a geometric shape that is complex and detailed in structure at any level of magnification. Fractals possess an inherent self-similarity or self-affinity in their geometric structures – that is, they have the property that each small portion of the fractal can be viewed as a reduced-scale replica of the whole.

The efforts of researchers around the world to combine fractal geometry with electromagnetic theory have led to new and innovative antenna designs. The properties of fractal can be exploited to develop antennas with multi-band operation [5] – [7]. The Sierpinski antenna is the first reported example of a fractal shape antenna with a multiband behavior. That is, an antenna that keeps a similar behavior (radiation patterns and input parameters) through several bands. The number of bands and their positions are strongly related to the antenna geometry, which demonstrates the tight link between the fractal nature of the antenna and its electromagnetic behavior.

If the fractal geometry properties are incorporated into the design of microstrip antenna, a smaller (compact size, light weight and thin profile), easier to fabricate and reliable antenna system for mobile communication can be produced. The complexity of the antenna system can be reduced, thus improving the communication service cost and quality.

2.5 Transmission Line Characteristic

One of the important characteristics linked with transmission lines is the way in which they can transform the impedance of a load into a different value at different length of the line. The impedance transformation formula is shown below:

$$Z_{in}(\ell) = Z_o \frac{Z_L + jZ_o \tan(\beta\ell)}{Z_o + jZ_L \tan(\beta\ell)}$$

where $\beta = \frac{2\pi}{\lambda}$ and ℓ is the length of the line. The relationship can be seen in terms of $\beta\ell = \frac{2\pi\ell}{\lambda}$. At $\ell = \lambda$ or $\ell = \frac{\lambda}{2}$, Z_{in} is just equal to the load impedance Z_L [4]. From this equation it can be seen that the input impedance varies with the length of the line.

2.6 Relationship of Microstrip Antenna Parameters

The shape of the microstrip patch antenna used in this project is rectangular and it is being fed using microstrip feed line (refer to Figure3-1 to Figure 3-4). Most of the parameters can be defined i.e. dielectric thickness (**d**), dielectric constant ($\in_r$) and air box height (**h**). Other parameters such as the width of the feed line, **w**, can be calculated (by approximation) using the equation below:

$$Z_o = \frac{120\pi d}{w\sqrt{\in_r}}$$

where characteristic impedance, Z_o is set to be 50Ω. The resonant frequencies are related to the length and width (**a** and **b**) of the rectangular patch (refer to Figure 3-4) by these set of equations:

$$L = \frac{\lambda_d}{2}$$

$$\lambda_d = \frac{\lambda}{\sqrt{\in_r}}$$

$$f = \frac{c}{\lambda}$$

where L represents **a** or **b**. λ_d is the effective wavelength with respect to the dielectric material and λ is the wavelength of the operating frequency. Finally, the frequency can be calculated using the speed of light, **c** divided by the wavelength.

The table below shows the antenna dimension, resonant frequency and wavelength calculated from the equations above.

Table 2-1: Antenna dimension and resonant frequency

Dimension of a & b ($\lambda_d/2$)	*Frequency*		λ
cm	*Hz*	*GHz*	*cm*
4	2587745848	**2.588**	11.593101
3.9	2654098305	**2.654**	11.303274
3.8	2723942997	**2.724**	11.013446
3.7	2797563078	**2.798**	10.723619
3.6	2875273164	**2.875**	10.433791
3.5	2957423826	**2.957**	10.143964
3.4	3044406879	**3.044**	9.8541362
3.3	3136661633	**3.137**	9.5643087
3.2	3234682309	**3.235**	9.2744811
3.1	3339026900	**3.339**	8.9846536
3	3450327797	**3.45**	8.6948261
2.9	3569304617	**3.569**	8.4049985
2.8	3696779782	**3.697**	8.115171
2.7	3833697552	**3.834**	7.8253434
2.6	3981147458	**3.981**	7.5355159
2.5	4140393356	**4.14**	7.2456884
2.4	4312909746	**4.313**	6.9558608
2.3	4500427561	**4.5**	6.6660333
2.2	4704992450	**4.705**	6.3762058
2.1	4929039710	**4.929**	6.0863782
2	5175491695	**5.175**	5.7965507
1.9	5447885995	**5.448**	5.5067232
1.8	5750546328	**5.751**	5.2168956

2.7 Scattering Parameters

The scattering parameters, often called as S parameters is a useful way to represent the port characteristics of RF (radio frequency) and microwave circuits. Consider a linear two-port network shown in the figure below.

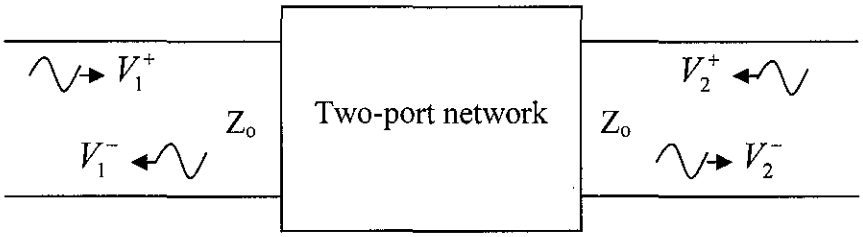

Figure 2-2: Two-port network ingoing and outgoing voltage waves

Both ports are transmission lines with characteristics impedance Z_o. For transmission lines, voltage waves can propagate in two directions. Let V_1^+ and V_1^- be the incoming and outgoing voltage phasors respectively at port 1. Similarly, V_2^+ and V_2^- are the incoming and outgoing voltage phasors respectively at port 2. The S parameters relate the waves as shown in the matrix equation below:

$$\begin{bmatrix} V_1^- \\ V_2^- \end{bmatrix} = \begin{bmatrix} S_{11} & S_{12} \\ S_{21} & S_{22} \end{bmatrix} \begin{bmatrix} V_1^+ \\ V_2^+ \end{bmatrix}$$

From the above equation, each S parameter can be expressed in terms of the ratio of outgoing and incoming voltage phasor.

$$S_{11} = \frac{V_1^-}{V_1^+} \text{ when } V_2^+ = 0 \text{ (Port 2 matched)}$$

$$S_{12} = \frac{V_1^-}{V_2^+} \text{ when } V_1^+ = 0 \text{ (Port 1 matched)}$$

$$S_{21} = \frac{V_2^-}{V_1^+} \text{ when } V_2^+ = 0 \text{ (Port 2 matched)}$$

$$S_{22} = \frac{V_2^-}{V_2^+} \text{ when } V_1^+ = 0 \text{ (Port 1 matched)}$$

Each S parameter is the ratio of an outgoing wave to an incoming wave under the restriction that one of the ports is terminated with a nonreflecting or matched load. From the equations above, S_{11} is just the reflection coefficient seen at port 1 when port 2 is terminated by a matched load. Similarly, S_{22} is just the reflection coefficient

seen at port 2 when port 1 is terminated by a matched load. The parameters S_{12} and S_{21} are not reflection coefficients. Rather, these parameters represent the coupling of waves from one port to the other [4].

The simulation results would be presented in the form of S_{11} magnitude (dB) vs. frequency plot[1]. At the resonance frequency, the reflection is minimum (maximum power is radiated to space) yielding high S amplitude in negative dB scale as presented in the figure below.

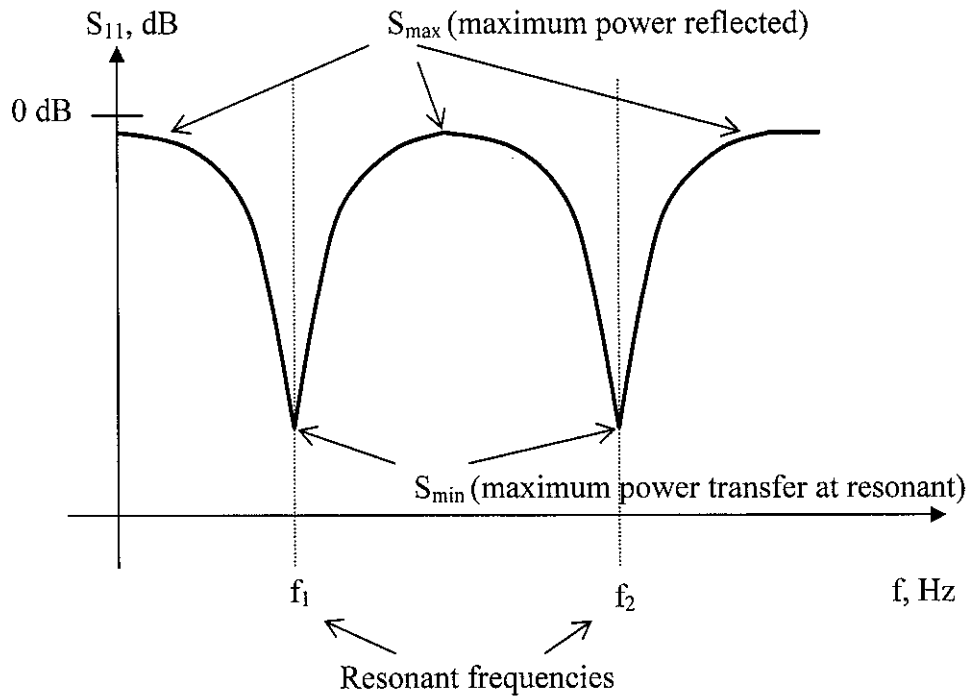

Figure 2-3: S-magnitude plot

[1] The term S-magnitude plot is used throughout the report for the sake of simplicity.

CHAPTER 3

METHODOLOGY

3 METHODOLOGY

The purpose of the project is mainly to investigate (using software simulation) the multiband behavior of microstrip antenna in terms of:

- Multiband characteristics and frequency separation of bands.
- Dependency of resonance frequency for various bands on dimensions and slot positions.
- Effect of feed location on the antenna behavior.

For the first semester, the main concerns were to verify HP HFSS in simulating microstrip antennas and analyzing typical rectangular microstrip antenna for multiband behavior. To achieve those objectives the author needs to be familiar with the concepts of microstrip and multiband antennas and as well as the HP HFSS simulation software.

For the second semester, two sets of simulations were done. The first set was to investigate the effect of changing the patch dimension and feed location. The second set emphasized on the effect of slot (window) introduced within the patch and also the effect when the slot position was varied.

Figure 3-1 below shows the microstrip antenna drawn in HP HFSS. The air box is needed by the simulation software for farfield calculation. The patch (including the feedline) and ground[2] are defined as conductor. The dielectric which is located between the patch and ground has permittivity of 2.1 (dielectric constant, $\in_r$) and loss

[2] located at the bottom plane and it has the same size as the dielectric accept for the thickness which is negligible in the simulation

tangent of 0.0003. The plane where the feedline touches the edge of the air box and dielectric is defined as the port (permits energy to flow into the antenna). The other planes except for the port and ground are defined as radiating boundary.

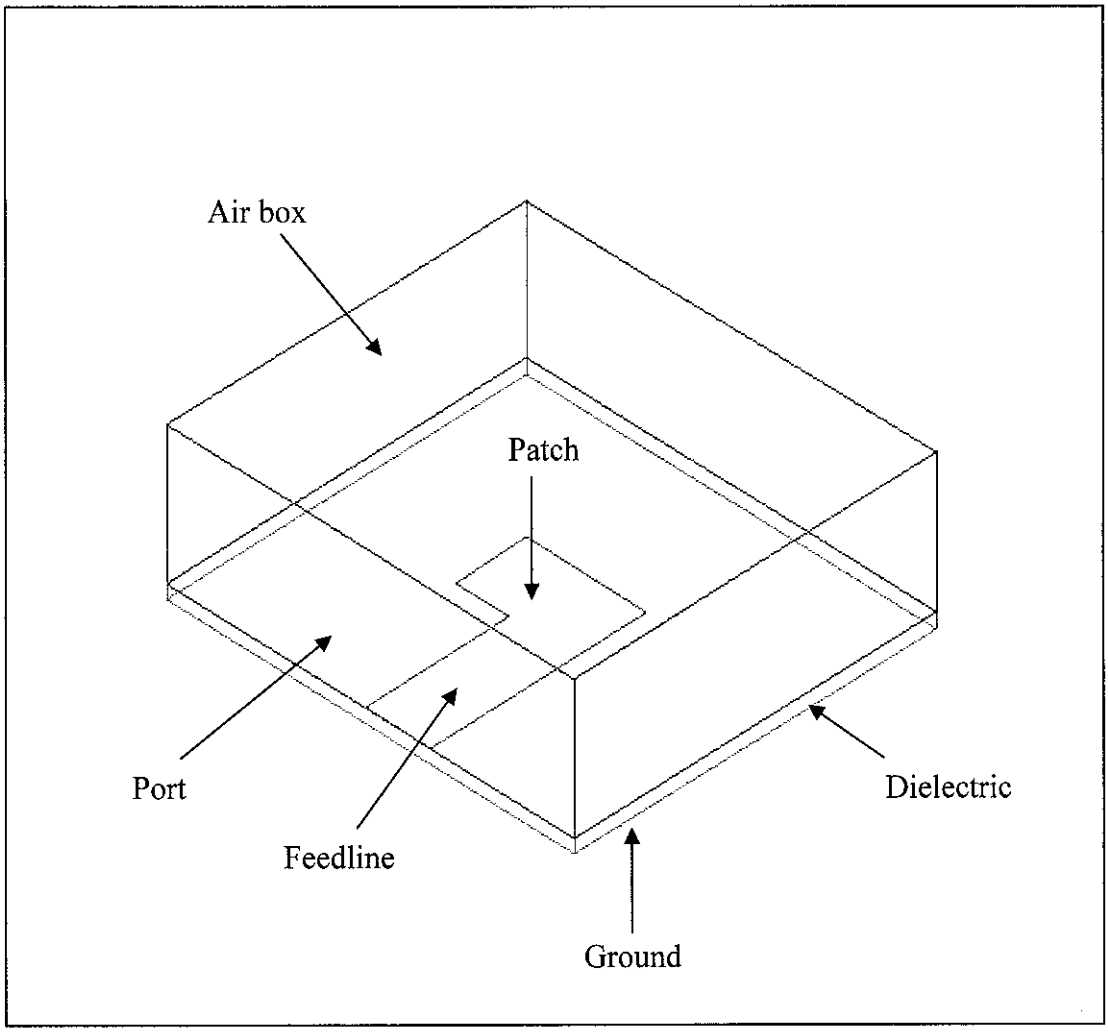

Figure 3-1: Microstip antenna drawn in HP HFSS

Figure 3-2 shows the top view of the structure. The separation between the edges of the patch to the edges of the dielectric is denoted by **S** as shown in Figure 3-2. The side view is shown in Figure 3-3.

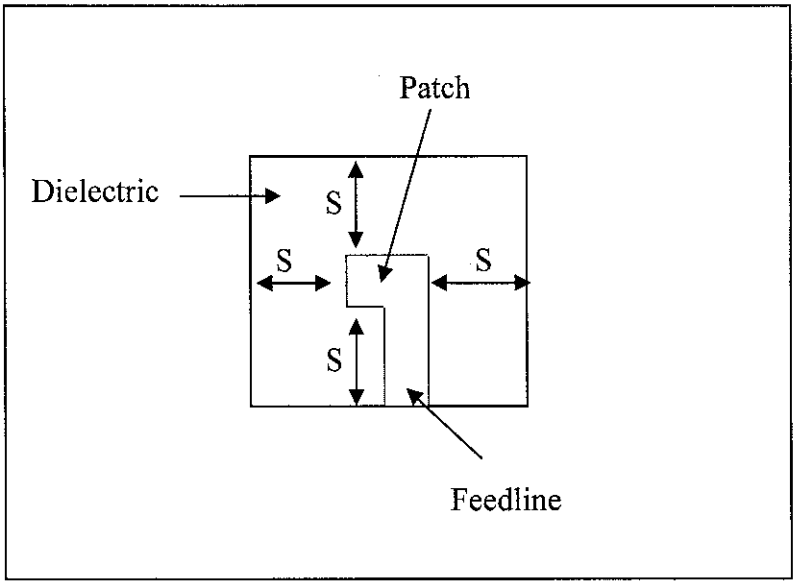

Figure 3-2: Top view

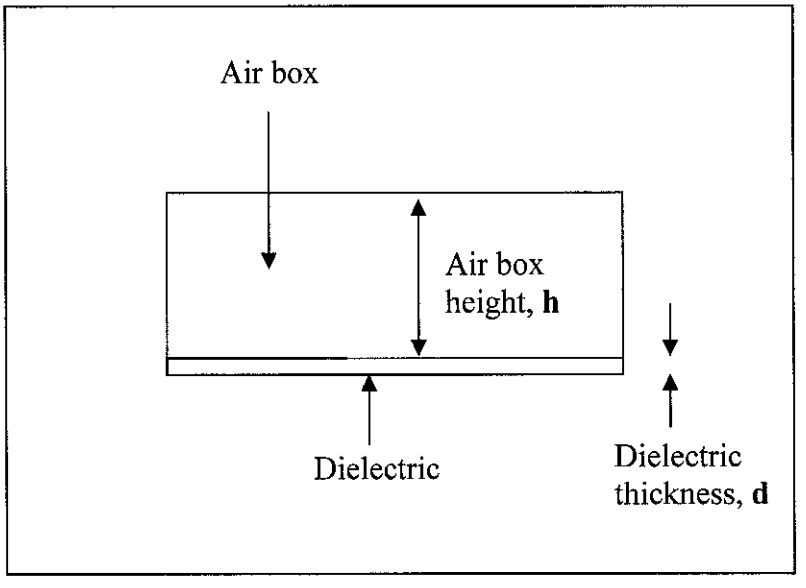

Figure 3-3: Side View

For the first set, the simulation was done using (refer to Figure 3-1 to Figure 3-4) **a** = 3 cm, **d** = 0.3175 cm, air box height, **h** = 10**d**, ϵ_r = 2.1, width of feedline, **w** = 1.65 cm (to get $Z_o = 50\Omega$, refer to equation in section 2.6) and the separation between the edges of the patch to the dielectric was taken to be at 2λ corresponding to side **a** (**S** =12 cm). The dimension of side **b** was not fixed and taken to be 1.8 cm, 2 cm, 2.5 cm and 2.8 cm. Thus, there would be four different patch dimensions to be used in simulation.

For each patch dimension, two sets of simulations would be done with the feedline located at Position 1 and Position 2 respectively (refer to Figure 3-4). Refer to section 4.1 for the results.

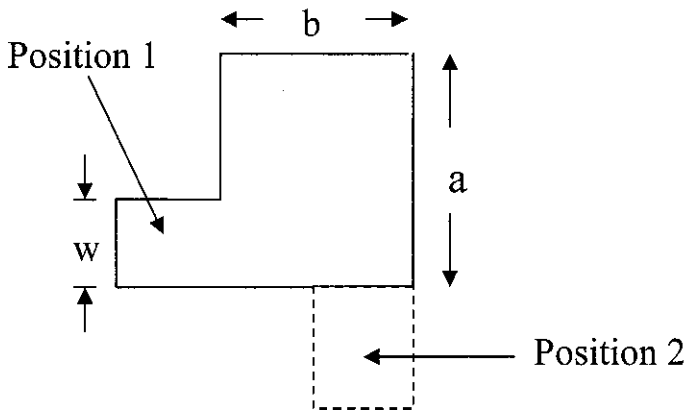

Figure 3-4: Two different feedline locations

The above situation was further investigated by narrowing down the choices of **a** and **b** dimensions. The dimension of **a** now is fixed to 3 cm and **b** is chosen to be at 1.8 cm. With this fix dimension, the antenna was simulated with the feedline located at the edge of the **a** and **b** sides as shown in Figure 3-5 (Case 1 and Case 2 respectively). More simulations were completed with the feedline moved towards the center of the patch and the results are shown in section 4.2.

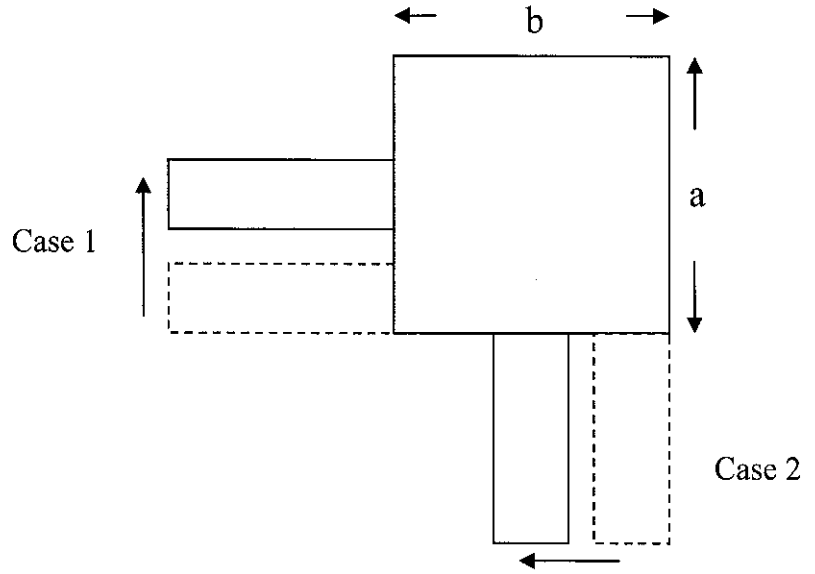

Figure 3-5: Changing feed locations

The second set of simulation introduces a *slot* [3] or *window* to the patch. Theoretically this should result in a shift in the resonant frequency or frequencies as compared with the result without the slot. With slot positioned, current will take a longer path to flow thus the antenna would have a larger effective dimension. Therefore, a microstrip antenna without slot can have the same resonant frequency with the ones with slot.

Another aspect to be investigated is the separation between the edges of the patch to the edges of dielectric denoted by **S** as shown in Figure 3-2 and Figure 3-6. To avoid fringing effect, **S** is normally chosen to be at least one λ. The next experiment investigates the effect of slot and also **S** to the resonant frequency of the antenna.

[3] The term slot and window are used interchangeably throughout the dissertation.

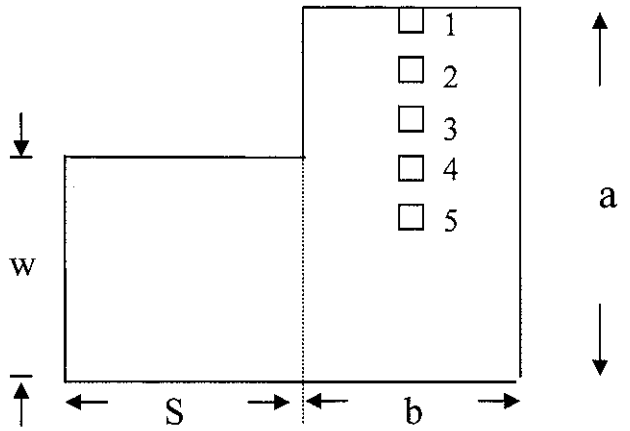

Figure 3-6: Example of 5 different positions of the slot

Referring to the Figure 3-6 above, **a** was chosen to be 3 cm, **b** = 1.8 cm, **d** = 0.3175, air box height, **h** = 3.175 cm, ϵ_r = 2.1 and **w** = 1.65 cm. There are four different dimensions of **S** to be investigated – one λ corresponding to **a** and **b** and also 2λ corresponding to **a** and **b**. Three positions for slot were chosen for each value of **S** – position 2, 3 and 4. The size of the slot was taken to be 0.1 of $\frac{a}{b}$ (0.3 cm x 0.18 cm). For each **S**, the antennas without slot are also simulated (total of 16 simulations). The simulation results are shown in section 4.3.

For the rest of the simulations, the separation between the edges of the patch to the edges of dielectric was taken to be at one λ corresponding to **b** (**S** = 3.6 cm, refer to Figure 3-2). This would consequently reduce the computing time taken for a simulation. The other dimensions would follow the ones mentioned in the previous paragraph. These dimensions were kept constant for the rest of the subsequent experiments described below.

Another set of simulations (refer to section 4.3) with 15 slot positions were also done. The slot was put in 15 different positions on the patch and simulated one by one. Also, the slot is positioned at the center of the patch and being enlarged – from 0.2 to 0.9 times the patch size. The results will be presented in section 4.5.

Further investigation continued with a new shape of window. The window used previously was rotated at 90° and combined to become a cross shape as shown in Figure3-7. Hypothetically this shape should result in shifts for both frequencies. The results for this investigation is shown in section 4.4. The same window shape (refer to Figure 3-7) with the size doubled was also investigated and the result is presented in section 4.5.

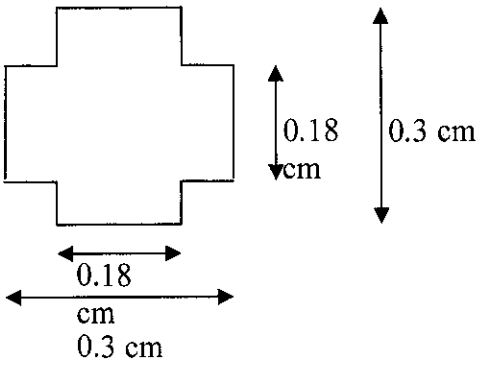

Figure 3-7: New window shape

Another aspect of investigation is the effect of window rotation. The window (rectangular) is positioned at the center of the patch and rotated by 20°, 30°, 40°, 45°, 60° and 90° (refer to Figure 3-8). The results of these simulations are presented in section 4.6.

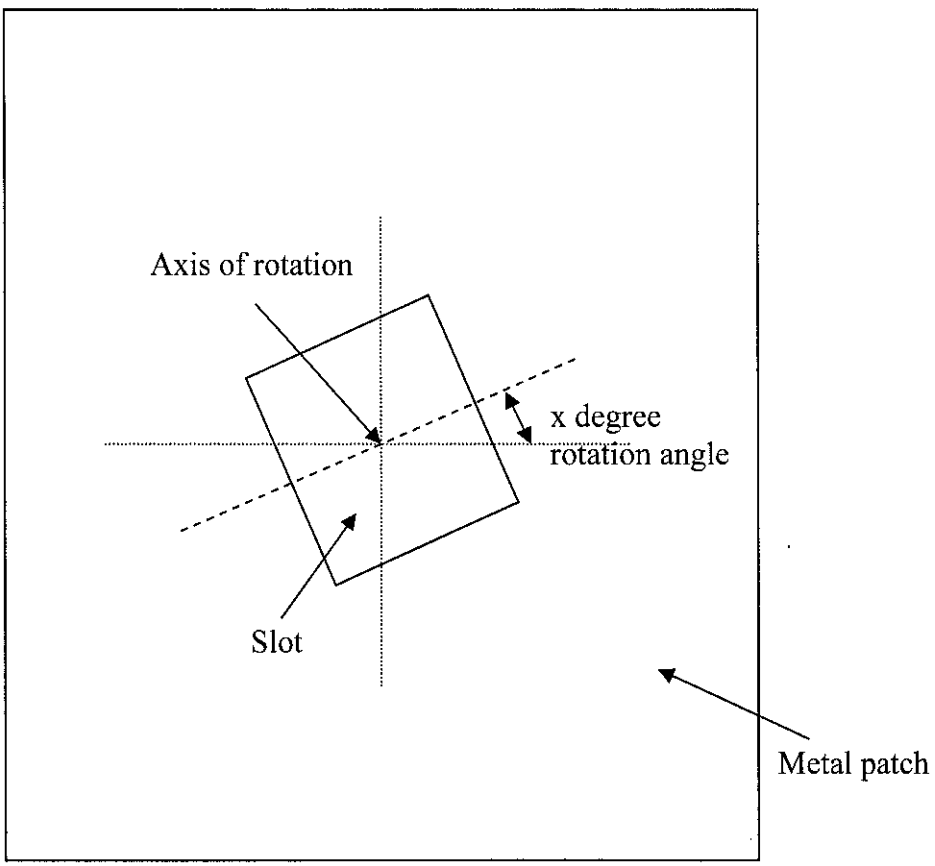

* Figure drawn not to the exact ratio

Figure 3-8: Rotating the slot

3.1 Tool

The tool used to analyze the multiband behavior of microstrip antenna is the HP High-Frequency Structure Simulator (HP HFSS) software. HP HFSS developed by the HP EEsof Division, is a complete solution for modeling arbitrarily shaped, passive 3-D structures. It is a general-purpose tool that can be used for a variety of electromagnetic (EM) modeling applications, including antenna design and analysis, machined-component design and analysis, circuit design and analysis and high-speed digital-circuit design and analysis.

HP HFSS computes:

- Scattering parameter (S-parameter) response for multiple modes.
- Electric field distributions, including far-field antenna radiation patterns.

- Impedance and propagation constants for multiple modes.

3.2 Using HP HFSS

The HP HFSS drawing interface (based on the industry-standard AutoCAD drawing tool) can be used to draw the geometry of any structure interested in modeling. A 3D geometry that was created in any of a number of industry-standard file formats can also be imported in.

The ports, materials, and boundaries of the structure need to be identified before solving for the electromagnetic fields at the specified frequencies and desired accuracy.

This section gives the steps for modeling the structure and analyzing its electromagnetic behavior using HP HFSS. The steps are summarized in the figure below and the explanations will be provided in the following descriptions:

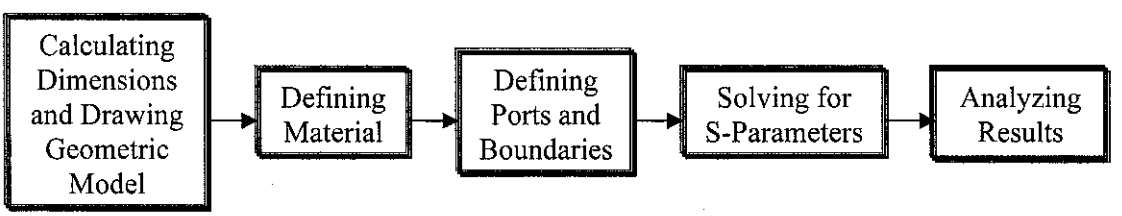

Figure 3-9: HP HFSS Modeling and Analysis Flow

3.2.1 Calculating Dimensions and Drawing the Geometric Model

First, some dimensions of the structure (microstrip antenna) need to be calculated using the relationship formulas (refer to 2.6) – the dielectric constant, operating frequency, ground plane dimensions, patch dimensions and characteristic impedance can be preset values. The structure can be drawn using the industry-standard, AutoCAD-based, drawing interface.

An unlimited number of undo steps allow user to back out of any drawing process, one step at a time. This final geometric drawing can be shaded and displayed from any angle and in a variety of colors for better visualization of the structure. If the structure contains commonly used parts, it can be quickly drawn by choosing objects from the standard parts library that comes with the software.

3.2.2 Defining Materials

The materials of which the structure is made can be defined while the structure is being drawn or after the structure is completed. The program allows user to choose from the supplied materials database or enter own materials, along with the appropriate parameters, such as permeability and permittivity, as well as conductivity if the material is a lossy metal, magnetic loss tangent and electric loss tangent if the material is a lossy dielectric and resistivity if the material is a resistor.

3.2.3 Defining Ports and Boundaries

The next step is to define the boundaries for the structure and also to define and calibrate the ports. Boundaries types include perfect magnetic or electric conductor, magnetic or electric symmetry boundary, a conductive boundary, a resistive boundary, a ground plane, or a radiation boundary.

Ports can be waveguides, coaxial connectors, or virtually any type of transmission line. The impedance, calibration and polarization lines for each port and mode of interest can also be drawn. The system solves and calculates the field solution for each port and provides useful data such as port impedance.

3.2.4 Solving for the S-Parameters

The simulator uses a mathematical technique known as finite element analysis to determine the field quantities and S-parameters. From the Solve dialog box, the user can choose to solve for the generalized scattering parameters at one adaptive frequency, for a frequency sweep, or for a fast frequency sweep.

S-parameters can be normalized with respect to the port impedances. If the S-parameters are to be included in a circuit simulation, they can be renormalized to 50 ohms with a simple menu command. An adaptive refinement of the finite-element mesh need to be performed to achieve results that fall within a user-specified accuracy.

A ports-only solution need to be specified for quick, 2D analysis of the ports of the structure. The fast frequency sweep is used for a quick preview of a structure's frequency response. This fast sweep saves time by solving the problem at a single frequency and then using a rational function approximation for the frequency bandwidth of interest.

3.2.5 Analyzing the Results

The post-processing features are used to display the numerical results and to display field distributions graphically after the simulation is complete and the S-parameters are calculated for the model. Port shading, surface shading, and plane shading provide a visual representation of wave propagation and electromagnetic characteristics on the computer screen.

Animated shaded field plots shift the phase at which the plot is shown, simulating the fields as they propagate through the structure in real time. These shaded plots can be rotated to gain various perspectives and an optimum viewing angle for the structure. User can display and print far-field, vector, and contour plots and graphs, and Smith Chart graphs, as well as tables of S-parameter data.

CHAPTER 4

RESULTS AND DISCUSSION

4 RESULTS AND DISCUSSION

The simulation results for the methods described in Chapter 3 are presented in this chapter.

4.1 Effect of Changing the Patch Dimensions and Feed Locations

For the patch configuration shown in Figure 3-4, the S-magnitude plots of the 8 simulations are shown below.

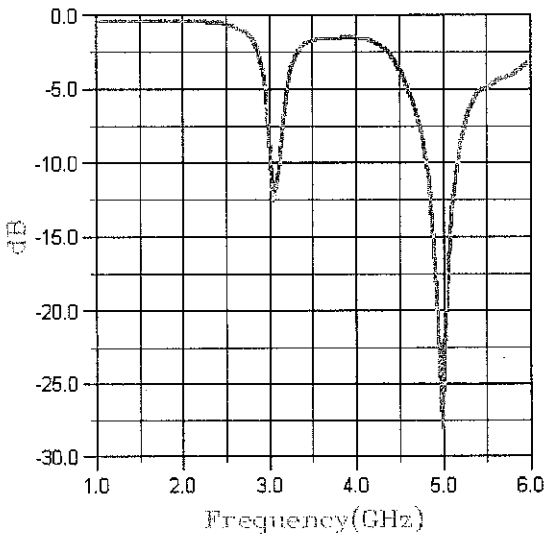

Figure 4-1: Simulation result when a = 3 cm, b = 1.8 cm and feedline at Position 1

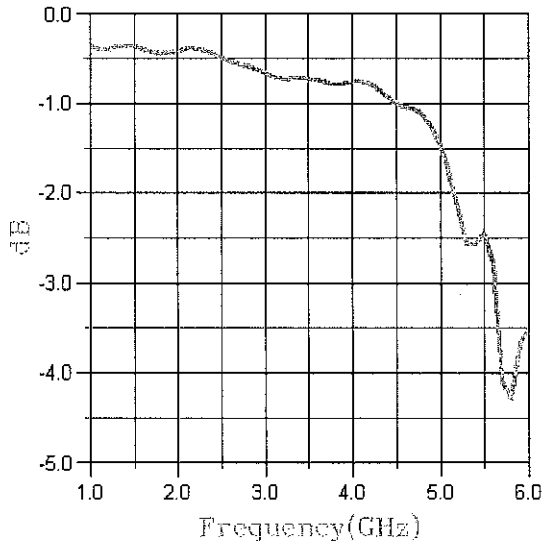

Figure 4-2: Simulation result when a = 3 cm, b = 1.8 cm and feedline at Position 2

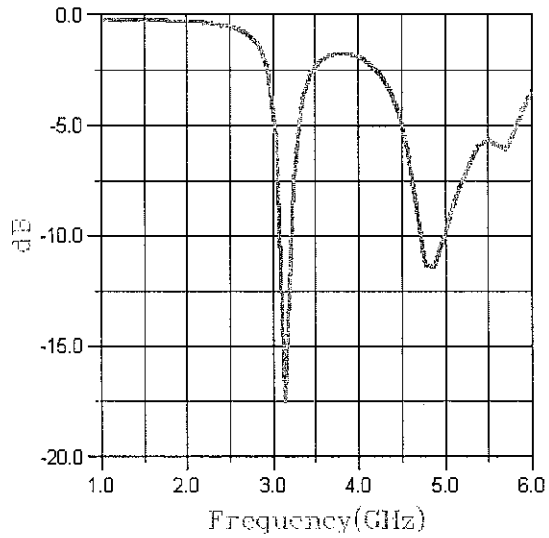

Figure 4-3: Simulation result when a = 3 cm, b = 2 cm and feedline at Position 1

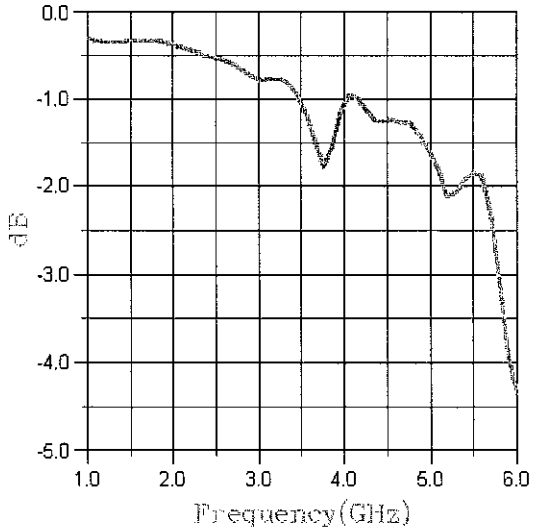

Figure 4-4: Simulation result when a = 3 cm, b = 2 cm and feedline at Position 2

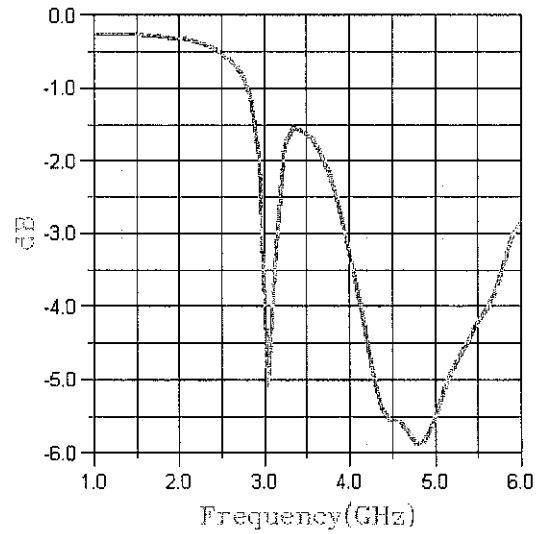

Figure 4-5: Simulation result when a = 3 cm, b = 2.5 cm and feedline at Position 1

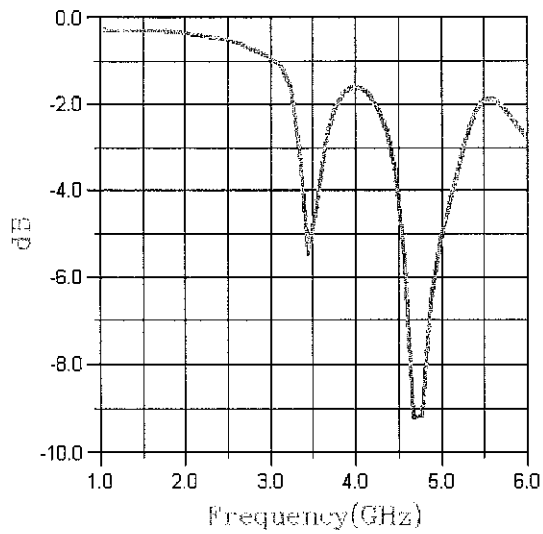

Figure 4-6: Simulation result when a = 3 cm, b = 2.5 cm and feedline at Position 2

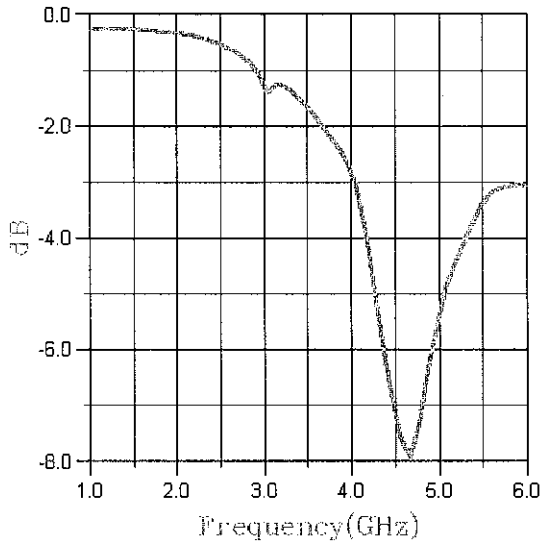

Figure 4-7: Simulation result when a = 3 cm, b = 2.8 cm and feedline at Position 1

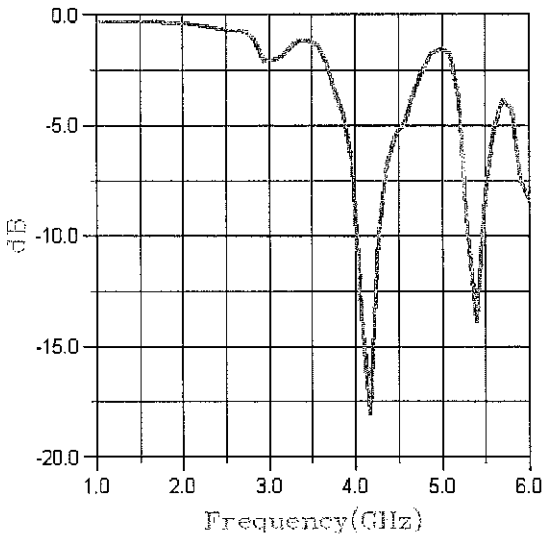

Figure 4-8: Simulation result when a = 3 cm, b = 2.8 cm and feedline at Position 2

As what can be observed from the results shown in Figure 4-1 to Figure 4-8, the resonant frequencies change when the dimension of **b** changes. When the feed location changes, the resonant frequencies also change.

When the feedline is located at Position 1, the graph in Figure 4-1 and Figure 4-3 show acceptable result but Figure 4-5 and Figure 4-7 are not showing the desirable

result. When the feedline is located at Position 2, the graph in Figure 4-6 and Figure 4-8 show acceptable result while Figure 4-2 and Figure 4-4 are not showing the desired result.

These results only show that the resonant frequencies, at which antennas radiated most efficiently, can be changed by arbitrarily changing the dimensions of the patch (with feedline positioned at certain location).

4.2 Varying Feedline

There were 2 sets of simulation done for this case. The first set investigates the effect of shifting the feed line from the edge to the centre of side **a**. The next set investigates the effect of shifting the feed line from the edge to the centre of side **b** (refer to Figure 3-5). The results are presented in the tables below:

Table 4-1: Resonant frequency when feedline is shifted along side a

Shift Location	f_1 *(GHz)*	f_2 *(GHz)*
0 (side)	3.1717	5.0707
1	3.1717	5.4343
2	3.1313	5.3939
3	3.0909	5.1919
4	3.1313	5.4343
5	3.0505	5.2727
6	3.0909	5.6768
7	3.0909	5.596
8	3.0505	5.6364
9	3.0909	5.8788
10 (centre)	none	5.9192

For the first set (corresponding to Case 1 in Figure 3-5), each location is shifted by 0.0675 cm. Refer to Appendix A for the S-magnitude plots.

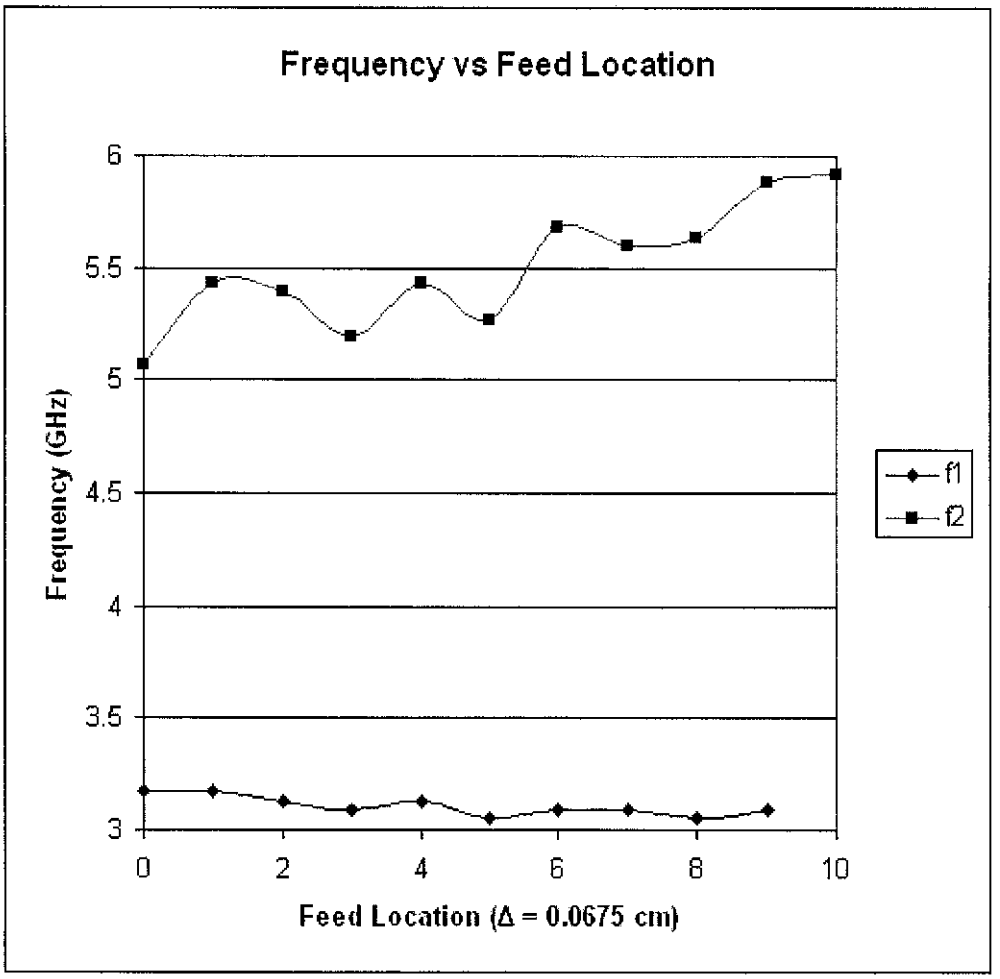

Figure 4-9: Resonant frequency vs. feed location plot (shifted along side a)

Table 4-2: Resonant frequency when feedline is shifted along side b

Shift Location	f_1 *(GHz)*	f_2 *(GHz)*
0 (side)	none	5.2323
1	none	5.2323
2	none	5.2323
3	none	5.1919
4	none	5.1515
5	none	5.2323
6	none	5.2323
7	none	5.2727
8	none	5.2727
9	none	5.2727
10 (centre)	none	5.2727

For the second set (corresponding to Case 2 in Figure 3-5), each location is shifted by 0.0075 cm. Refer to Appendix B for the S-magnitude plots.

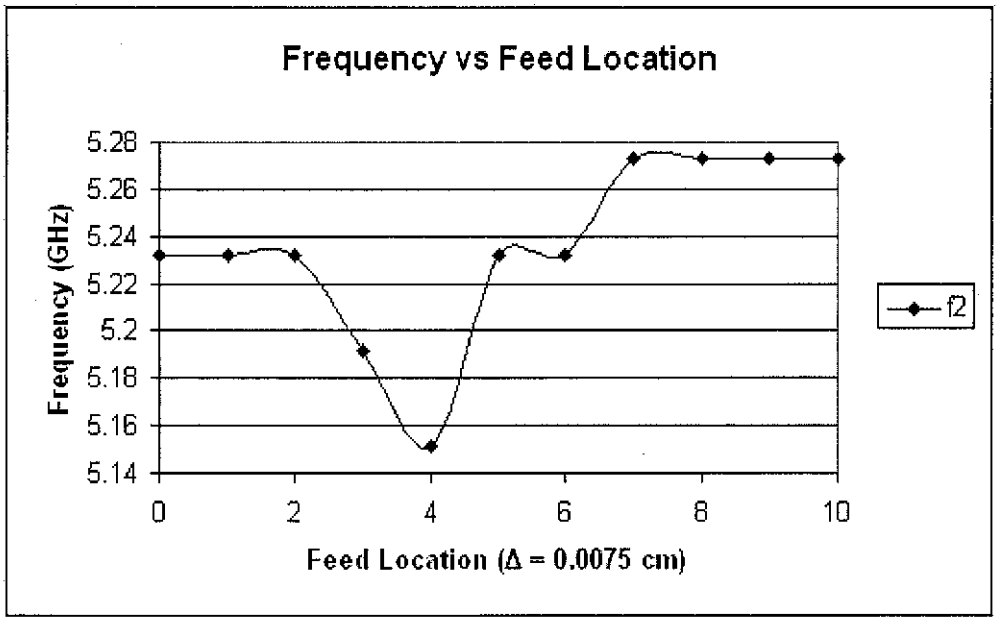

Figure 4-10: Resonant frequency vs. feed location plot (shifted along side b)

4.3 Effect of Slot within the Patch and Varying the Slot Position

Referring to Table 2-1, the calculated resonant frequencies for **a** = 3 cm and **b** = 1.8 cm are 3.45 GHz and 5.751 GHz. The resonant frequencies for the antenna with or without slot for four different values of **S** are tabulated in Table 4-3 below.

Table 4-3: Effect of the dimension of S

Description	*S = 3.6 cm*		*S = 6 cm*		*S = 7.2 cm*		*S = 12 cm*	
Slot	f_1 (GHz)	f_2 (GHz)	f_1 (GHz)	f_2 (GHz)	f_1 (GHz)	f_2 (GHz)	f_1 (GHz)	f_2 (GHz)
No window	3.1717	5.0707	3.2245	5.102	3.2121	5.0303	3.2245	5.1837
Location 2	3.1717	5.3131	3.2245	5.102	3.1717	5.0707	3.1429	5.1837
Location 3	3.1717	4.9899	3.0612	4.7755	3.1313	4.8687	3.2245	5.3469
Location 4	3.1313	4.9495	3.1429	4.8571	3.2121	4.9899	3.2245	5.2653

* refer to Figure 3-6 for the slot location and Appendix C for the S-magnitude plots.

From Table 4-3, the resonant frequencies of the antenna without slot when **S** = 12 cm are the nearest to the calculated value (f_1 = 3.2245 GHz and f_2 = 5.1837 GHz). The result did not show that the bigger the **S** value, the closer the resonant frequencies to

the calculated values. When slots are introduced, the resonant frequencies change for some slot locations at some values of **S** as compared to the ones without the slot.

Theoretically, with slot introduced within the patch, current will take a longer path through the patch, thus the antenna will effectively has a larger dimension (**a** and **b**). This will result in a smaller value of resonant frequencies. However these results do not correlate to the previous justification. Note that the location of the slot is not important as for now as it is merely placed to see whether the resonant frequencies will be shifted as compared to the ones without slot. The effect of the slot locations will be investigated and shown later.

For the rest of the simulations, **S** is chosen to be at 3.6 cm so that the computational time needed to run the simulation can be shortened. A total of 15 positions of windows were chosen as shown in Figure 4-11 below to investigate the effect of slot position to the resonant frequency of the antenna. The window was moved along a straight line (**b**/2) parallel to side **a**. For every simulation, the window is moved by 0.187 cm. The results of the 15 simulations are shown in Table 4-4 and Figure 4-12 below. Refer to Appendix D for the S-magnitude plots.

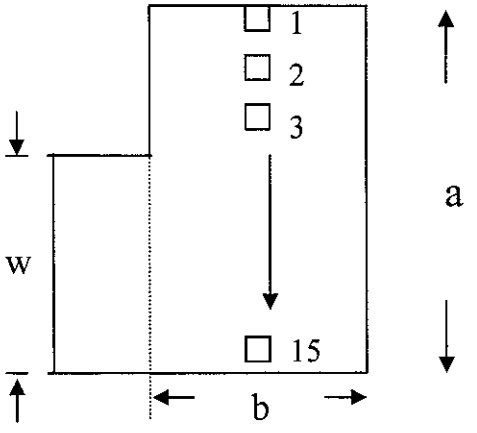

Figure 4-11: Window moved along b/2 line parallel to side a

Table 4-4: Resonant frequencies for different window position

Position	Relative Position of Center of Window to a	f_1(GHz)	f_2(GHz)
1 (top)	0.4375	3.1717	5.3131
2	0.375	3.1717	5.3131
3	0.3125	3.1717	5.2727
4	0.25	3.1717	4.9899
5	0.1875	3.1717	5.1919
6	0.125	3.1313	4.9495
7	0.0625	3.0909	4.8687
8 (center)	0	3.1717	4.9495
9	-0.0625	3.1717	5.3131
10	-0.125	3.1717	5.0707
11	-0.1875	3.1313	4.9495
12	-0.25	3.1717	5.3131
13	-0.3125	3.0909	4.7071
14	-0.375	3.1717	5.3131
15 (bottom)	-0.4375	3.1717	5.3131

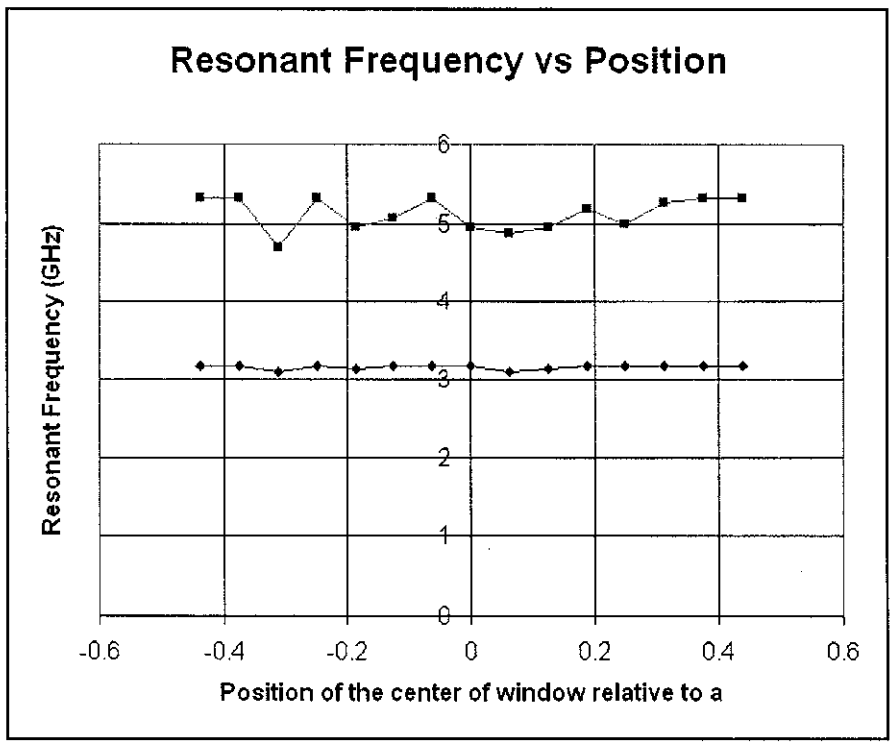

Figure 4-12: Resonant frequency vs. window position plot

With the slot positioned, the variation in frequency f_1 is from 3.0909 GHz to 3.1717 GHz, while the variation in f_2 is from 4.7071 GHz to 5.3131 GHz as is obvious in the Table 4-4.

Simulations with the window positioned along the **a**/2 line parallel to side **b** (as shown in Figure 4-13) was done to see whether f_1 would be shifted more. Taking the center of the patch as reference, the center of the window at position 3 is 0.225 cm away. Similarly, the center of the window at position 2 and position 3 are 0.45 cm and 0.675 cm away respectively.

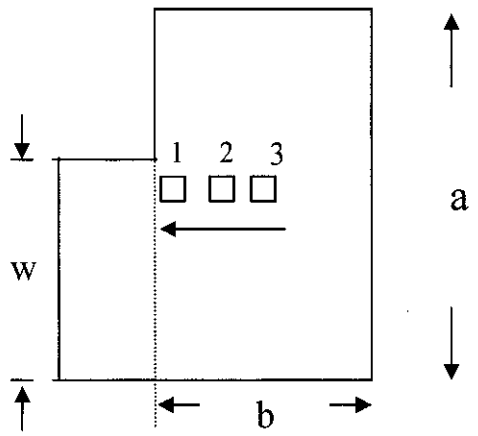

Figure 4-13: Window moved along a/2 line parallel to side b

The S-magnitude plots for the 3 positions are shown below:

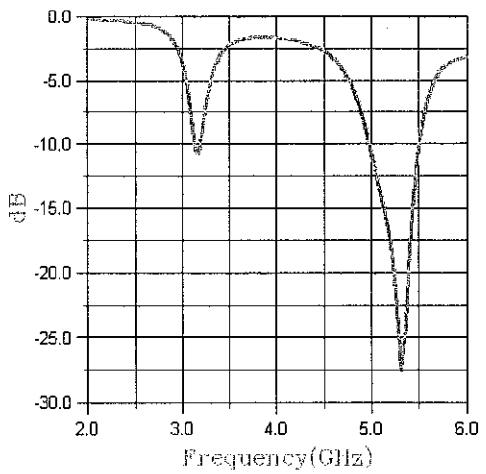

Figure 4-14: Window at position 1

From Figure 4-14, two resonant frequencies obtained were 3.1313 GHz and 5.3131 GHz.

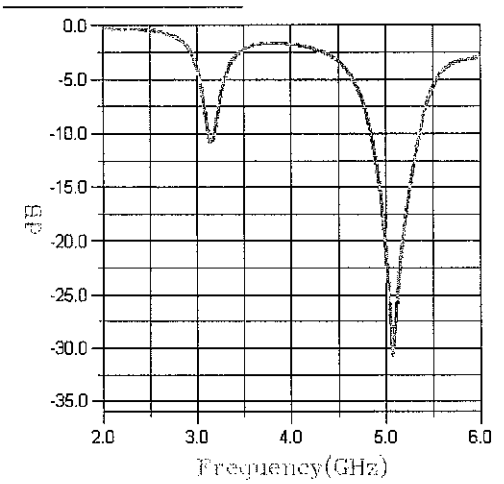

Figure 4-15: Window at position 2

From Figure 4-15, two resonant frequencies obtained were 3.1717 GHz and 5.0707 GHz.

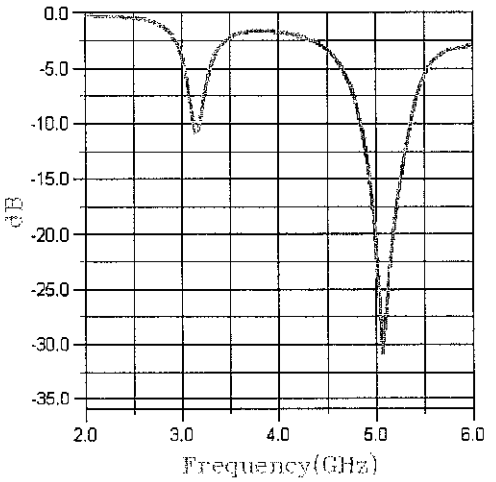

Figure 4-16: Window at position 3

From Figure 4-16, two resonant frequencies obtained were 3.1717 GHz and 5.0707 GHz. From the three S-magnitude plots, the resonant frequencies only shifted when the slot is placed at position 1. This means that there is no significant shift in f_1 when the window was moved along **a** and **b** sides.

4.4 New Window Shape

When the window shown in Figure 3-7 is used and located at the center of the patch, the S-magnitude plot is shown below:

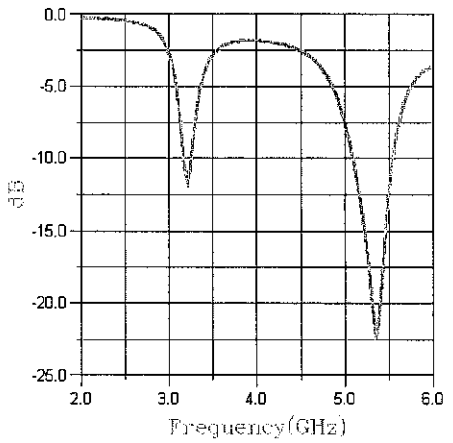

Figure 4-17: New window shape at center of patch

From Figure 4-17, two resonant frequencies obtained were 3.1717 GHz and 5.3535 GHz. From this result, it is shown that the first frequency component is still unshifted. However, more simulations need to be done for different locations before any conclusion can be made.

4.5 Window Size

Table 4-5 shows the results when the rectangular window is positioned at the center of the patch and the size is varied. Refer to Appendix E for the S-magnitude plots.

Table 4-5: Resonant frequencies for different window size

Slot size (a x b) relative to patch size (3 x 1.8 cm²)	*a* (cm)*	*b* (cm)*	*f_1 (GHz)*	*f_2 (GHz)*	*f_3 (GHz)*
0.1	0.3	0.18	3.1717	4.9495	-
0.2	0.6	0.36	3.0909	4.7475	-
0.3	0.9	0.54	3.0101	4.7071	-
0.4	1.2	0.72	3.0505	5.1515	-
0.5	1.5	0.9	3.0101	5.2323	-
0.6	1.8	1.08	2.8485	5.0303	-
0.7	2.1	1.26	2.8081	5.1111	5.8384
0.8	2.4	1.44	2.6465	4.9495	5.7172
0.9	2.7	1.62	2.6061	4.8283	-

When the window's size is changed from 0.1 to 0.9 times the patch size, the third resonant frequency component appears at window size of 0.7 and 0.8 times the patch size. Note that patch length a = 3 cm corresponds to resonant frequency of 3.45 GHz and b = 1.8 cm correspond to 5.75 GHz. These values are obtained by calculation used for estimation purpose (refer to Table 2-1). If at least one of the dimension of the window (a* and/or b*) has the length between 1.8 to 3 cm, the corresponding resonant frequency would be somewhere between 3.45 to 5.75 GHz.

The next simulation result shows the S-magnitude plot when the same window in Figure 3-7 with the size doubled is used. This window is placed at the same location as the simulation in section 4.4.

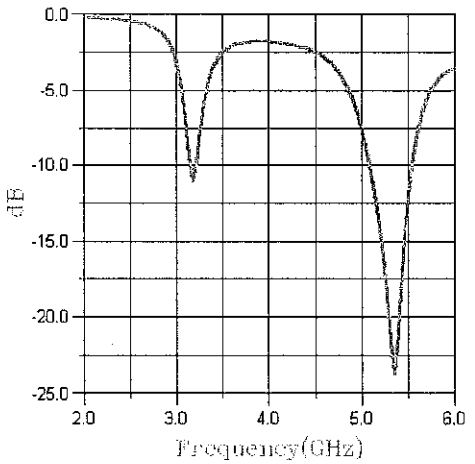

Figure 4-18: New window shape with dimensions doubled at center of patch

From Figure 4-18, two resonant frequencies obtained were 3.1717 GHz and 5.3535 GHz. Figure 4-17 and Figure 4-18 show that both simulations produced the same resonant frequency for both frequency components. At this point, the results obtained are insufficient. More results from other locations are needed for section 4.4 and 4.5 to arrive at a conclusion.

4.6 Window Rotation

The window is positioned at the center of the patch and rotated by 20°, 30°, 40°, 45°, 60° and 90°. Refer to Figure 3-8 for the illustration. The simulation result is shown below. Refer to Appendix F for the S-magnitude plots.

Table 4-6: Resonant frequencies for rotated window

Angle of Rotation	f_1 *(GHz)*	f_2 *(GHz)*
0°	3.1717	4.9495
20°	3.1717	5.0707
30°	3.1717	5.1919
40°	3.1313	4.8687
45°	3.1717	5.0707
60°	3.1717	5.0707
90°	3.1717	5.0707

From Table 4-5, at 30° rotation, the second frequency component f_2 shifted from 4.9495 GHz to 5.1919 GHz as compared to the unrotated window. At 40° rotation, both frequency components were shifted. At 20°, 45°, 60° and 90° rotation, both frequency components remained the same as the antenna without window (refer to section 4.3). Rotating the window at a certain angle can be another method of controlling the resonant frequency of a microstrip antenna with window already positioned within the patch.

CHAPTER 5

CONCLUSION AND RECOMMENDATION

5 CONCLUSION AND RECOMMENDATION

Rectangular microstrip antenna with microstrip feedline (Figure 3-1) is shown to exhibit multiband operation. The simulation results showed an obvious connection between the dimensions of the patch and the feed location to the S-magnitude plot or the multiband characteristics of microstrip antenna.

Also the resonant frequencies of the microstrip antenna can be shifted by introducing the slot or window within the patch. This provides a mean to control the value of the resonant frequency at constant patch dimension by manipulating the slot position, orientation and size. Therefore, the dependency of the resonant frequencies of microstrip antenna to the patch dimension can be reduced with the presence of slot.

The investigation was restricted to limited number of patch sizes due to time constraint. However, the results obtained can be applicable to rectangular patch microstrip antennas with sizes in terms of their **a** to **b** ratio (refer to Figure 3-4) equal to the investigated cases. With more investigations on the effect of slot, microstrip antennas can be designed given the separation of frequency as the specification.

Further enhancement to the project in the future can include the integration of these aspects – patch dimensions (**a** and **b**), feed locations and slot variation – to provide proper direction to microstrip antenna design. The scope of the project could be broaden to include investigations on other patch shapes and slots manipulation that could produce more than two effective resonant frequencies. The studies on microstrip antennas polarization is also a possible field to be explored.

REFERENCES

[1] Wayne Tomasi, 2001, "Electronic Communications Systems: Fundamentals Through Advanced", 4th Edition, Prentice Hall International, Inc.

[2] Ramesh Garg, Prakash Bhartia, Inder Bahl, Apisak Ittipiboon, 2001, "Microstrip Antenna Design Handbook", 1st Edition, Artech House, Inc.

[3] Constantine A. Balanis, 1997, "Antenna Theory: Analysis and Design", 2nd Edition, John Wiley & Sons, Inc.

[4] Kenneth R. Demarest, 1998, "Engineering Electromagnetics", 1st Edition, Prentice Hall Inc.

[5] Steven R. Best, 2002, "On the Significance of Self-Similar Fractal Geometry in Determining the Multiband Behaviour of the Sierpinski Gasket Antenna", IEEE Antennas and Wireless Propagation Letters, Volume 1

[6] Douglas H. Werner and Suman Ganguly, February 2003, "An Overview of Fractal Antenna Engineering Research", IEEE Antennas and Propagation Magazine, Volume 45, No. 1, pp38-57

[7] Carles Puente-Baliarda, Rafael Pous and Angel Cardama, April 1998, "On the Behavior of the Sierpinski Multiband Fractal Antenna", IEEE Transaction on Antennas and Propagation, Volume 46, No. 4, pp517-524

APPENDIX A

S-magnitude plots – Shifting the feed line from the edge to the centre of side a

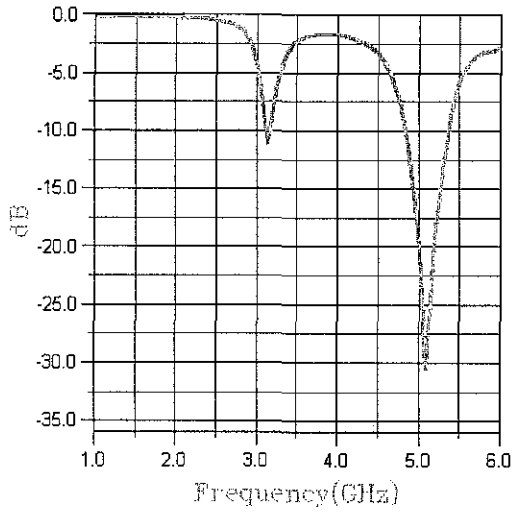

Figure A-5-1: Position 0

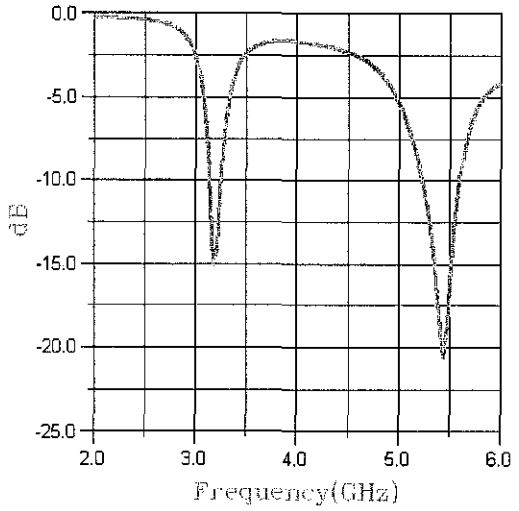

Figure A-2: Position 1

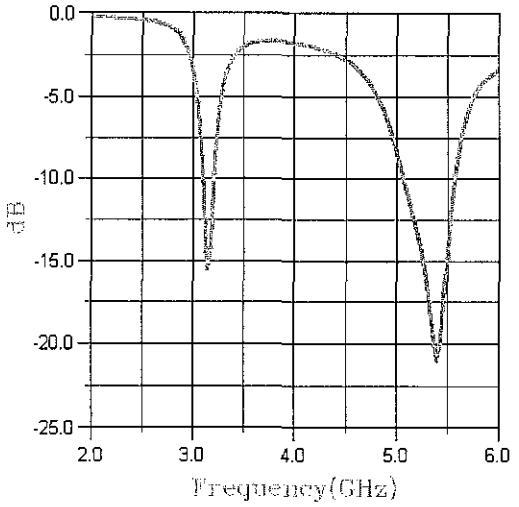

Figure A-3: Position 2

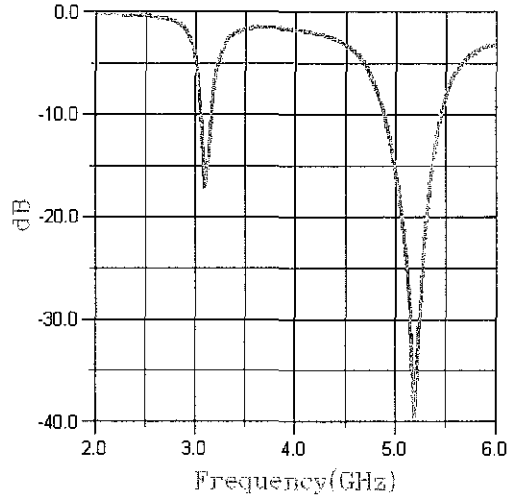

Figure A-4: Position 3

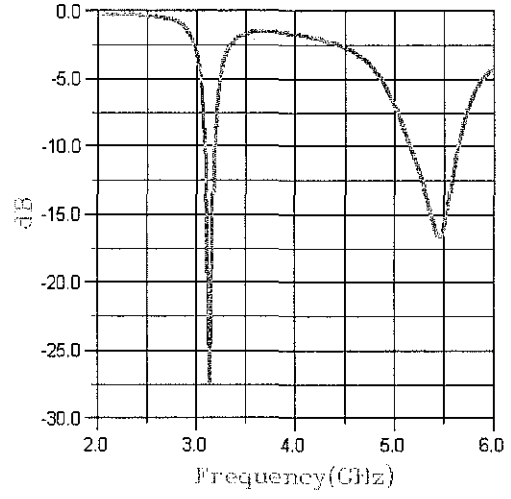

Figure A-5: Position 4

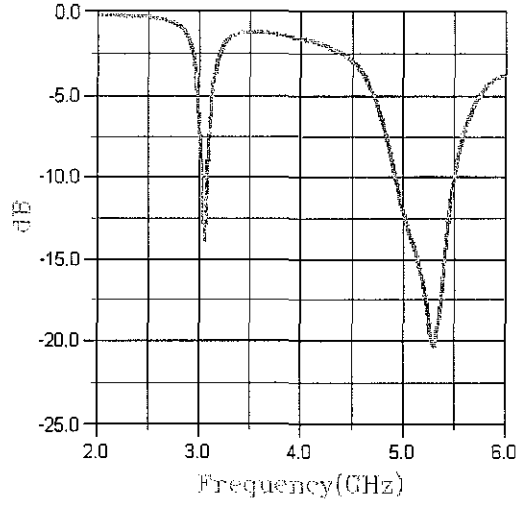

Figure A-6: Position 5

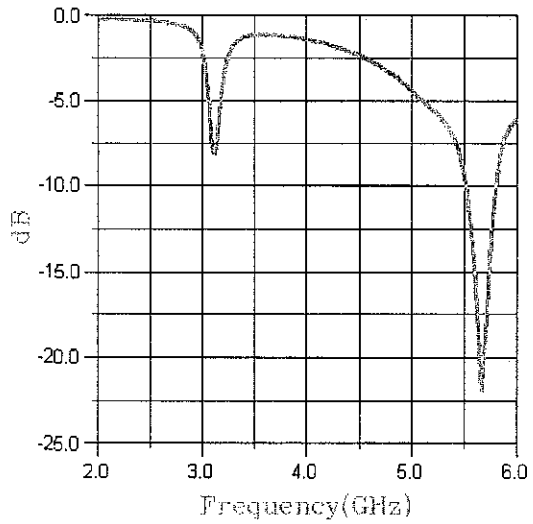

Figure A-7: Position 6

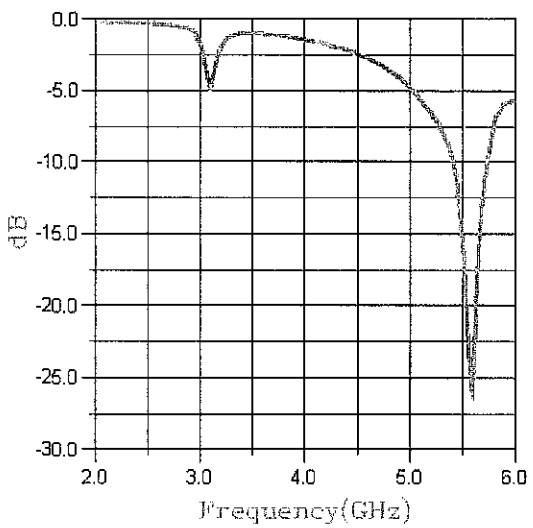

Figure A-8: Position 7

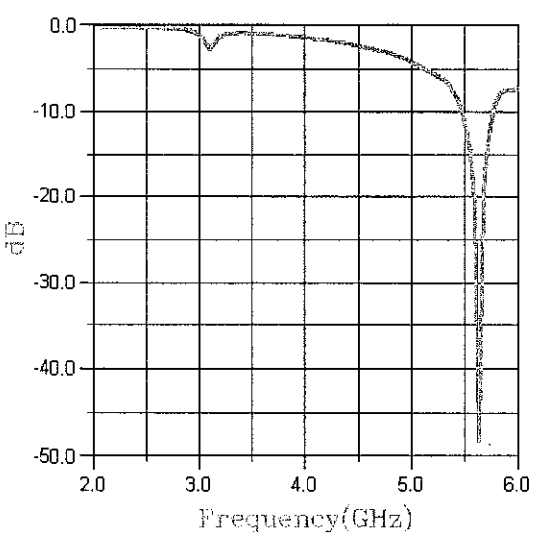

Figure A-9: Position 8

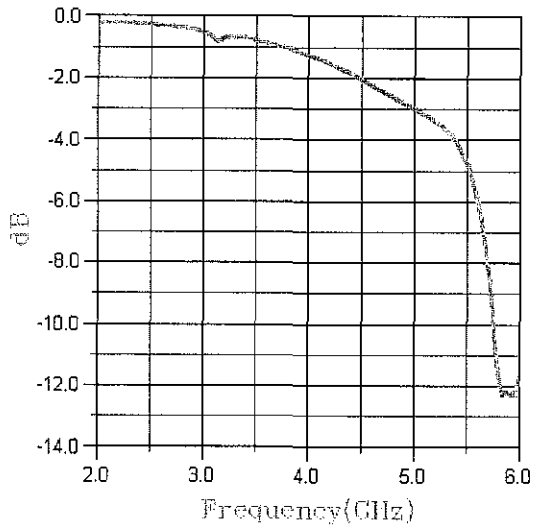

Figure A-10: Position 9

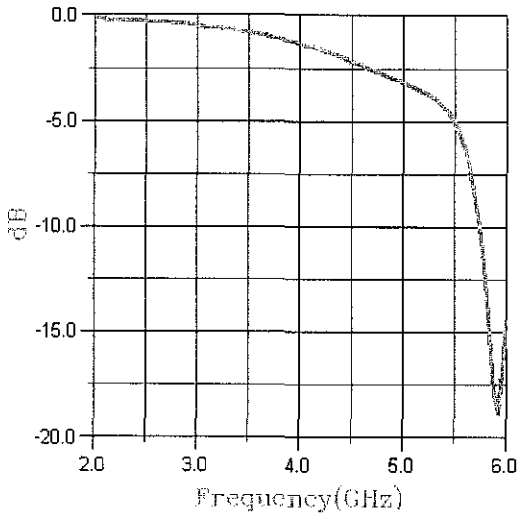

Figure A-11: Position 10

APPENDIX B

S-magnitude plots – Shifting the feed line from the edge to the centre of side b

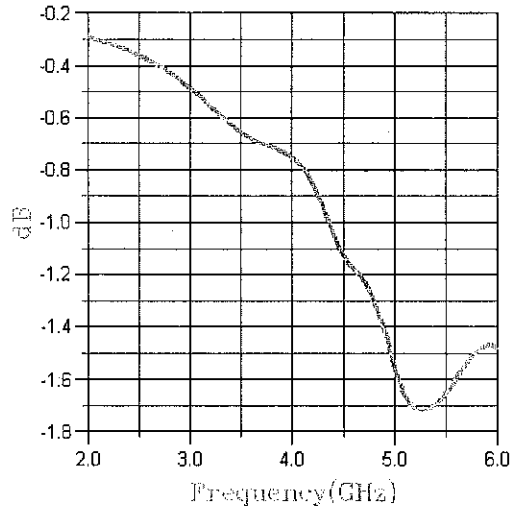

Figure B-1: Position 0

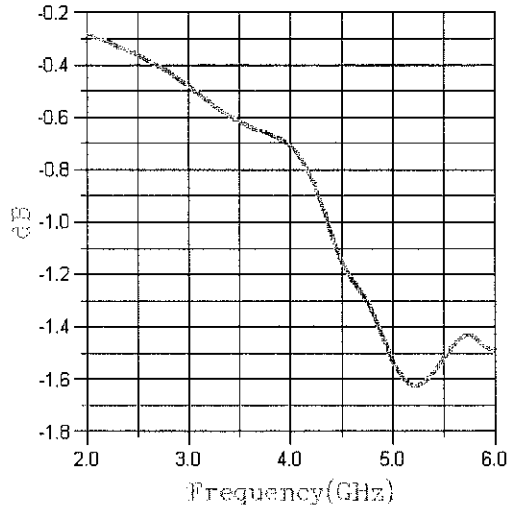

Figure B-2: Position 1

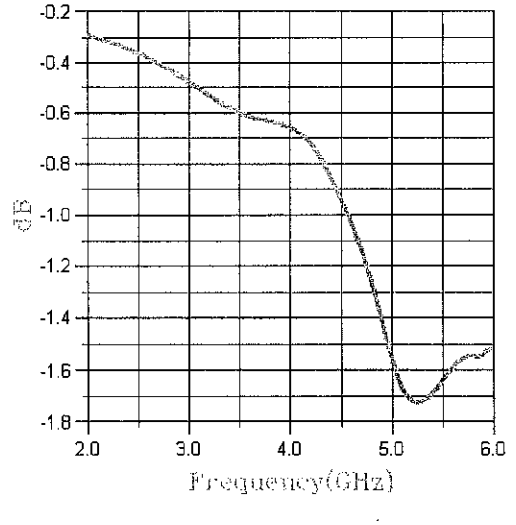

Figure B-3: Position 2

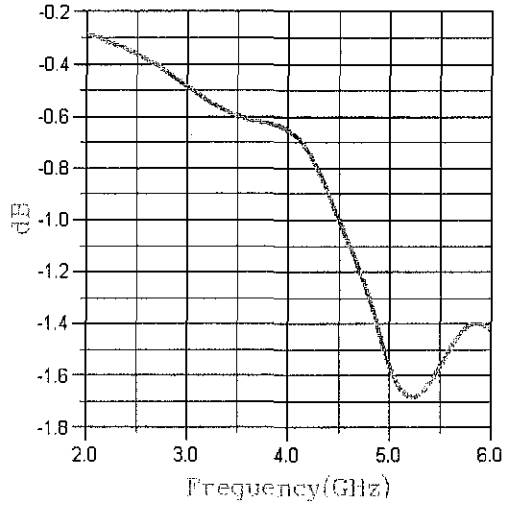

Figure B-4: Position 3

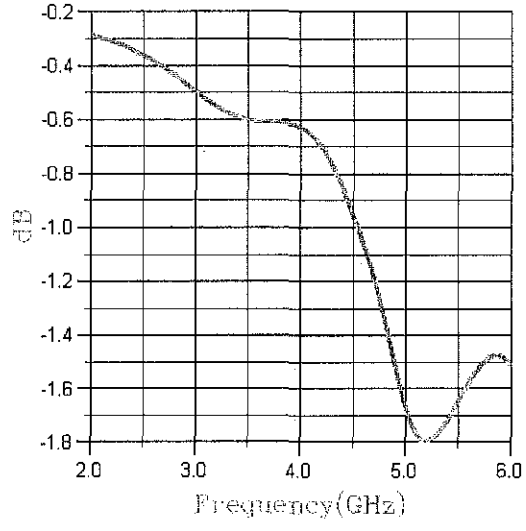

Figure B-5: Position 4

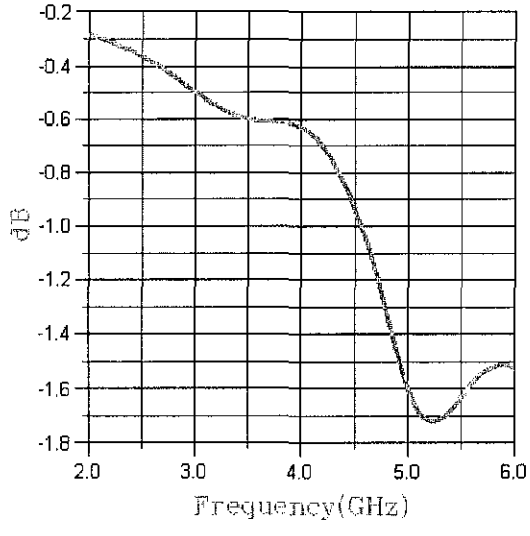

Figure B-6: Position 5

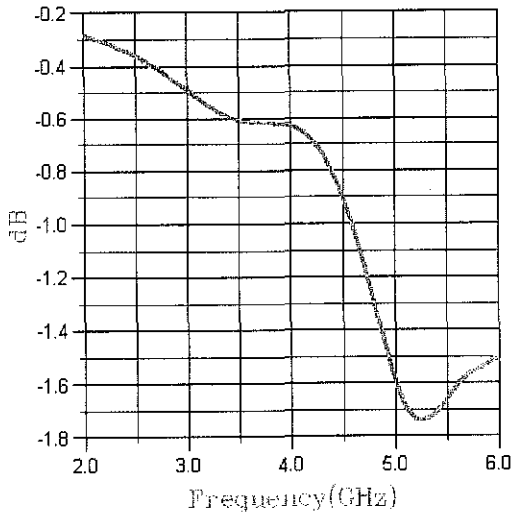

Figure B-7: Position 6

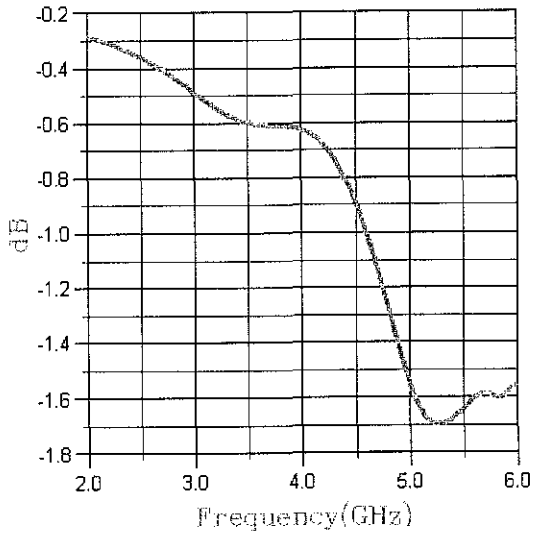

Figure B-8: Position 7

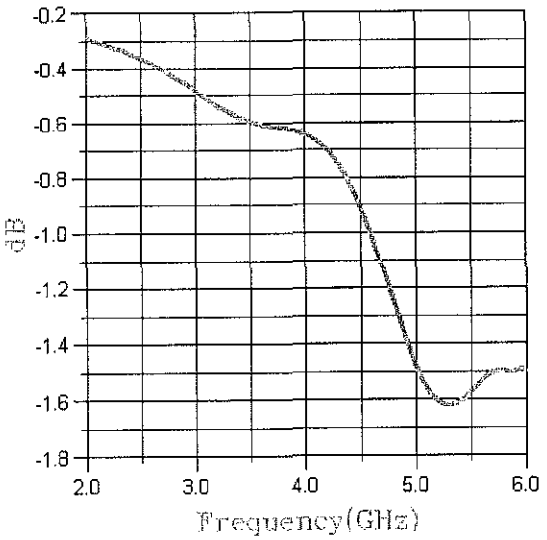

Figure B-9: Position 8

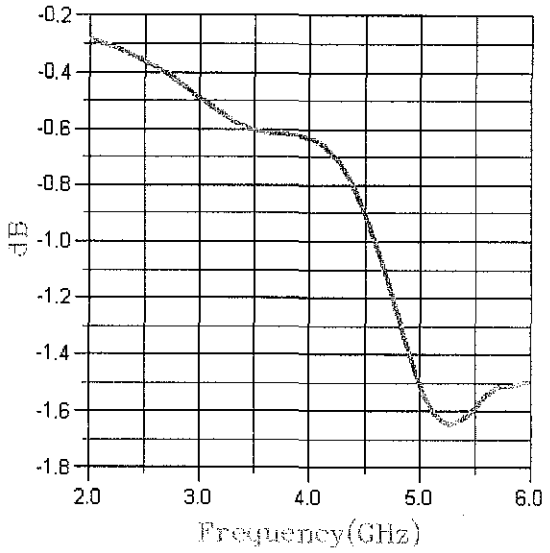

Figure B-10: Position 9

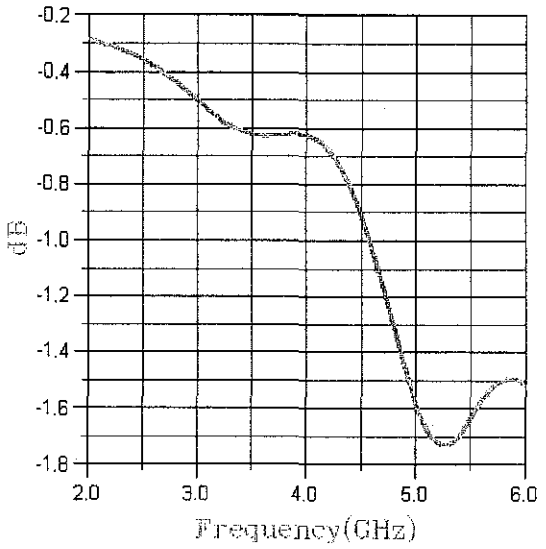

Figure B-11: Position 10

APPENDIX C

S-magnitude plots – Effect of separation between the edges of the patch to the edges of dielectric

One λ corresponding to b or S = 3.6 cm (side a = 3 cm and side b = 1.8 cm)

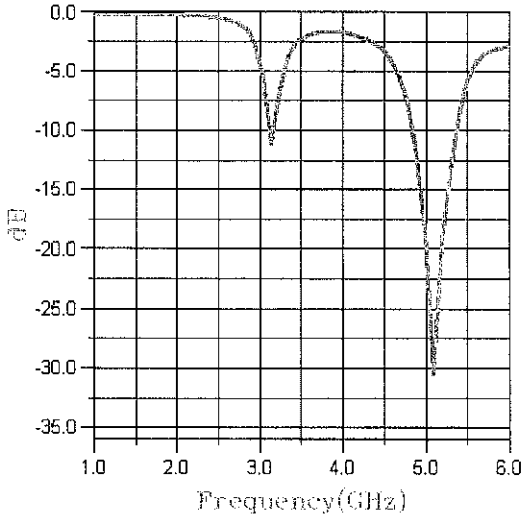

Figure C-1: Without window

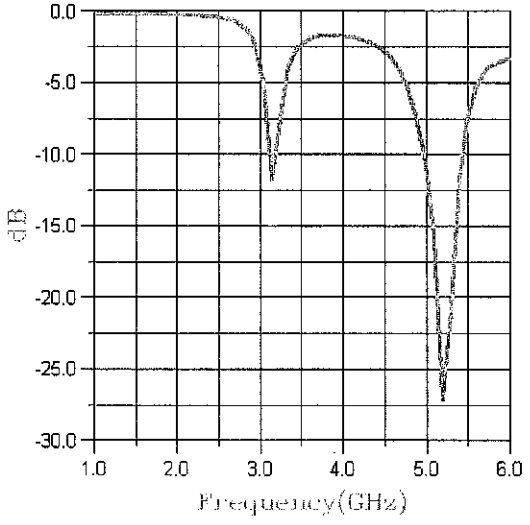

Figure C-2: Location 2

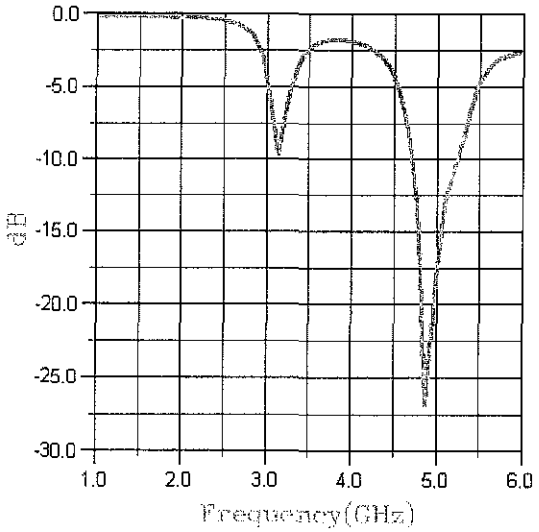

Figure C-3: Location 3

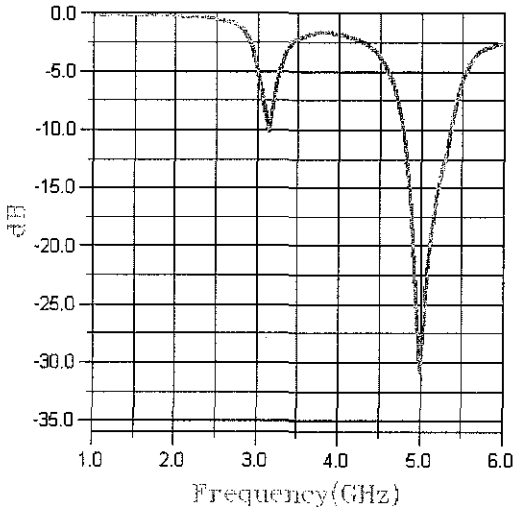

Figure C-4: Location 4

2 λ corresponding to b or S = 7.2 cm

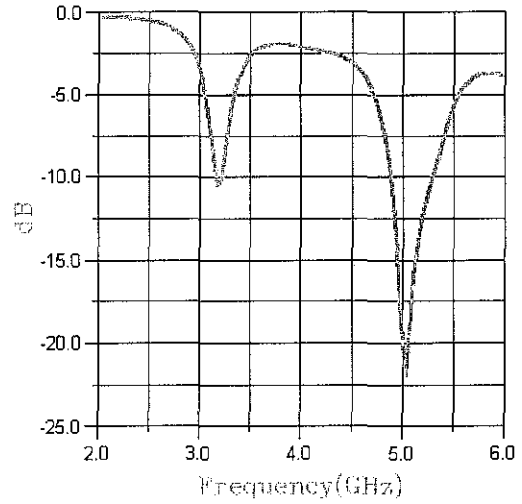

Figure C-5: Without window

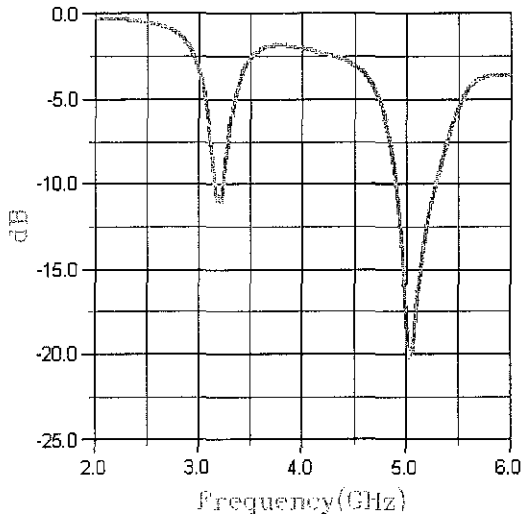

Figure C-6: Location 2

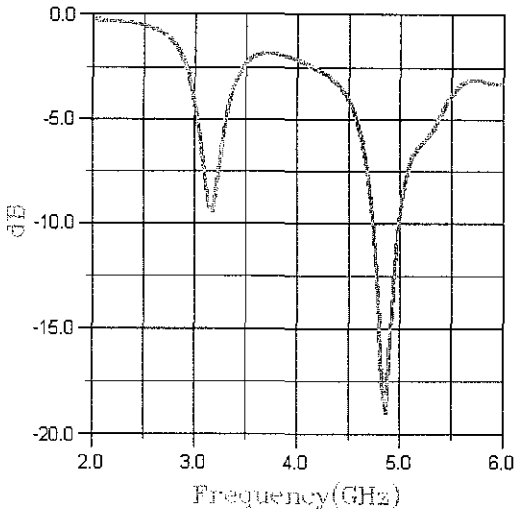

Figure C-7: Location 3

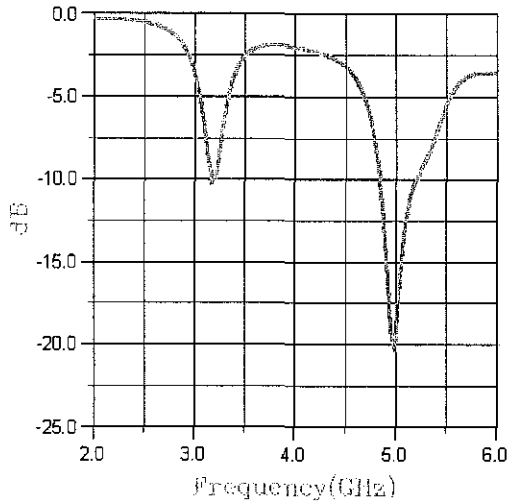

Figure C-8: Location 4

One λ corresponding to a or S = 6 cm

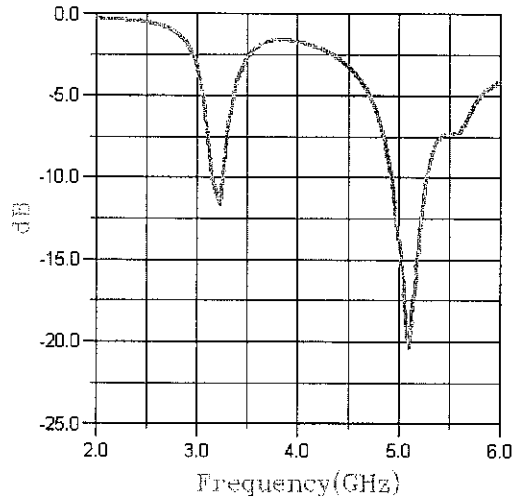

Figure C-9: Without window

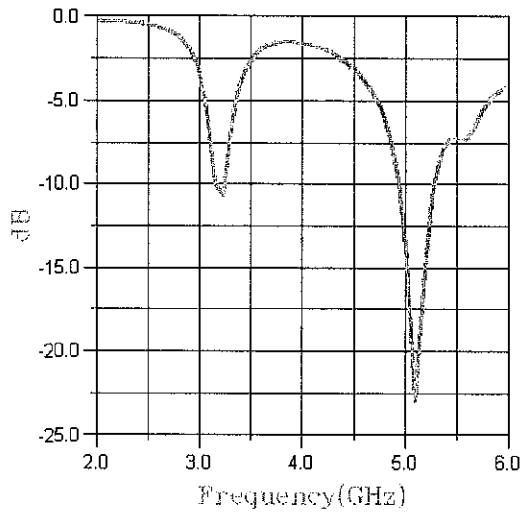

Figure C-10: Location 2

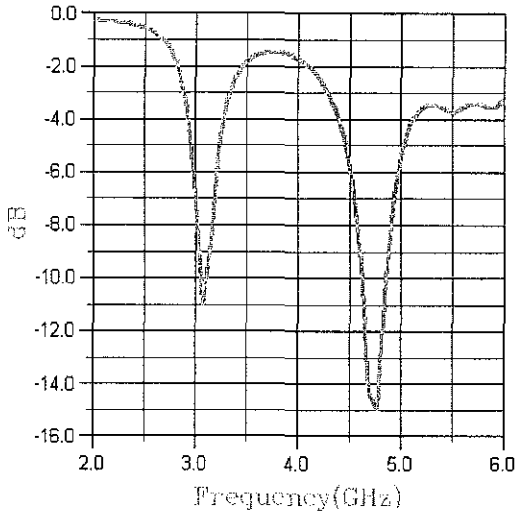

Figure C-11: Location 3

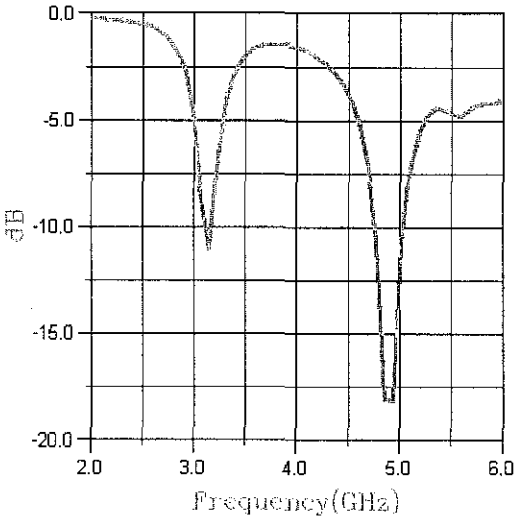

Figure C-12: Location 4

2 λ corresponding to a or S = 12 cm

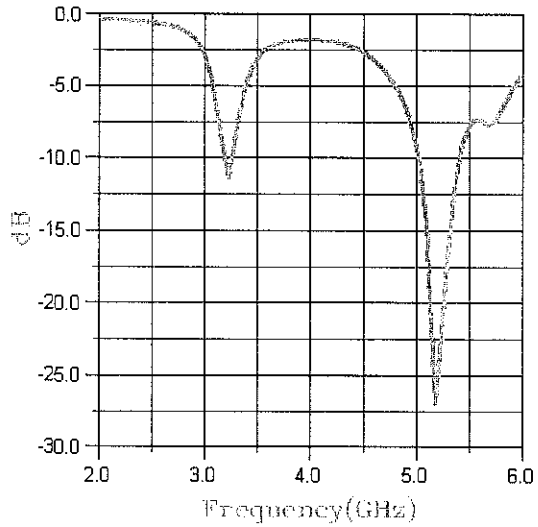

Figure C-13: Without window

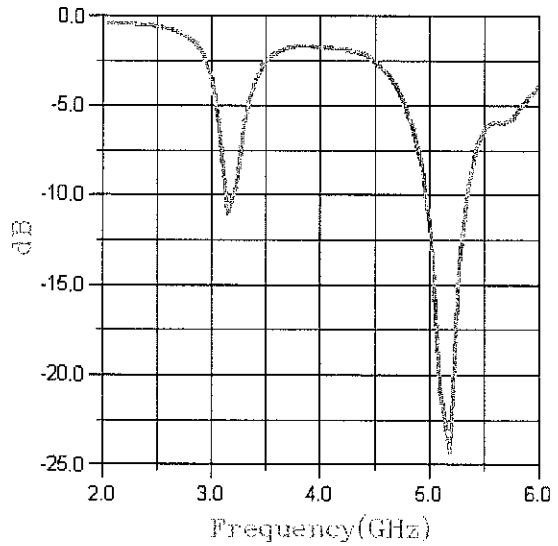

Figure C-14: Location 2

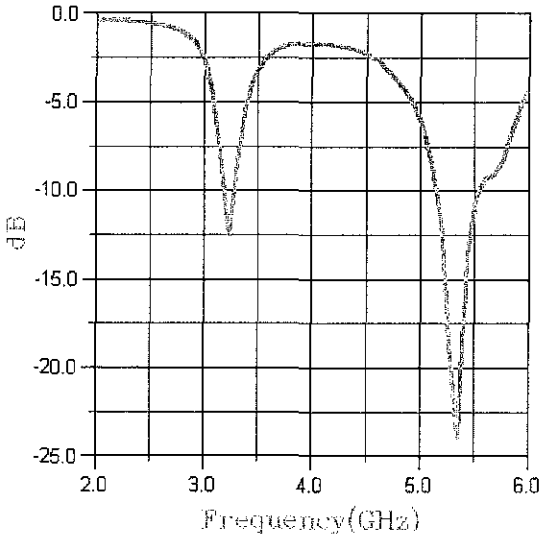

Figure C-15: Location 3

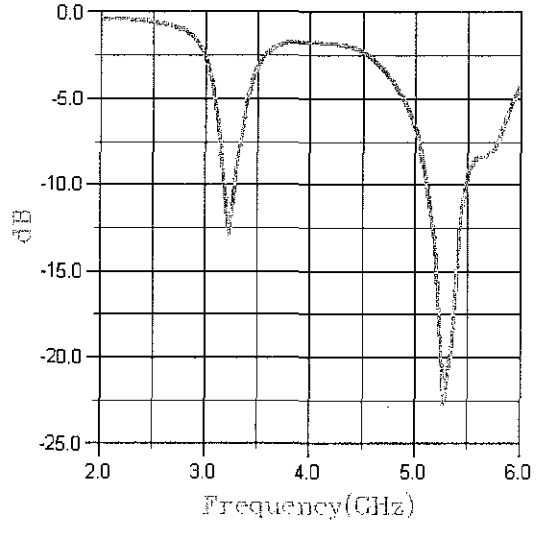

Figure C-16: Location 4

APPENDIX D

S-magnitude plots – Effect of varying slot position

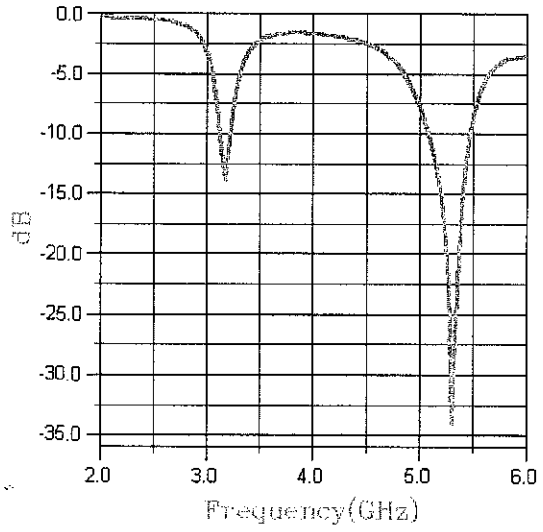

Figure D-1: Position 1

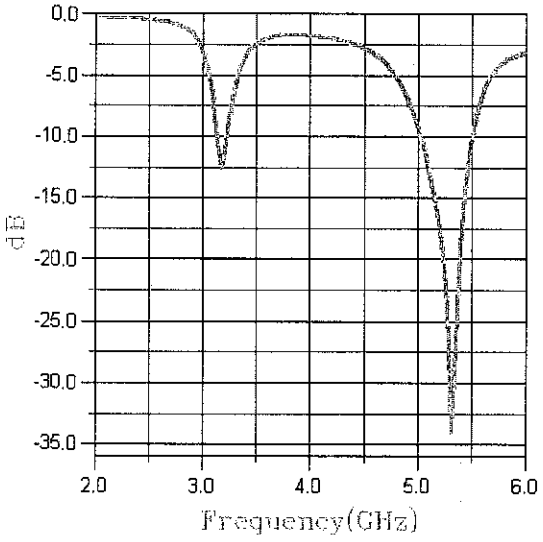

Figure D-2: Position 2

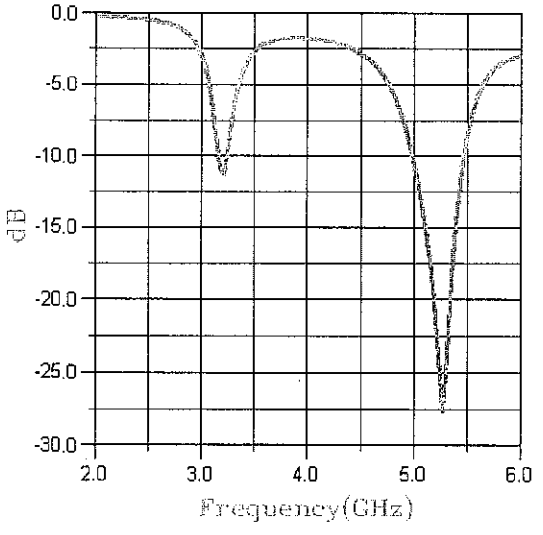

Figure D-3: Position 3

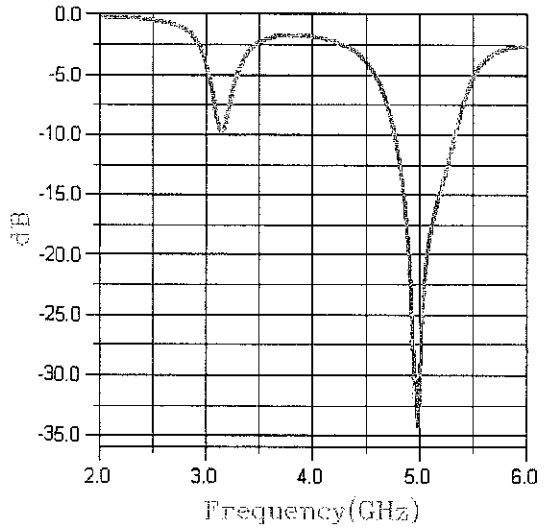

Figure D-4: Position 4

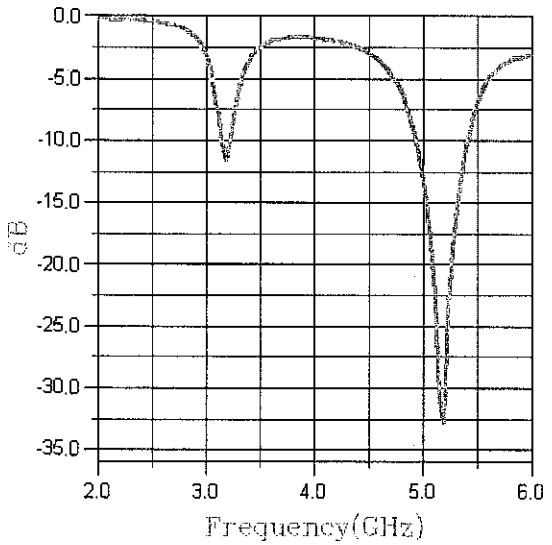

Figure D-5: Position 5

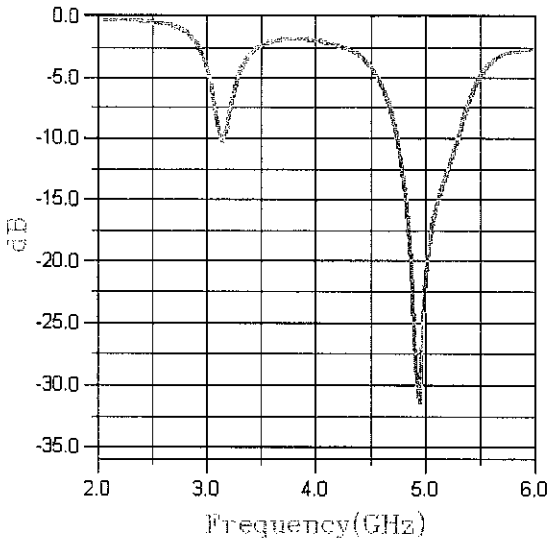

Figure D-6: Position 6

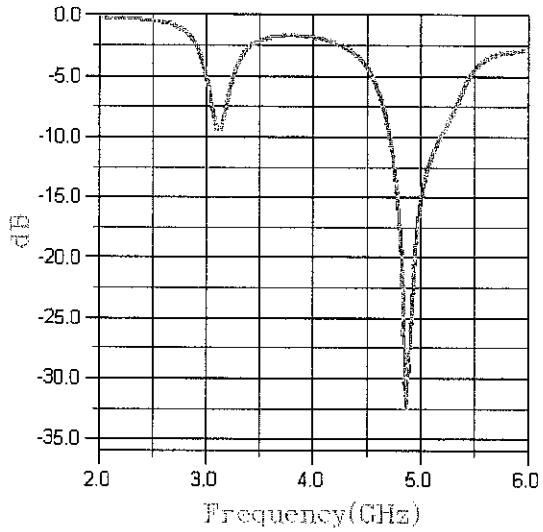

Figure D-7: Position 7

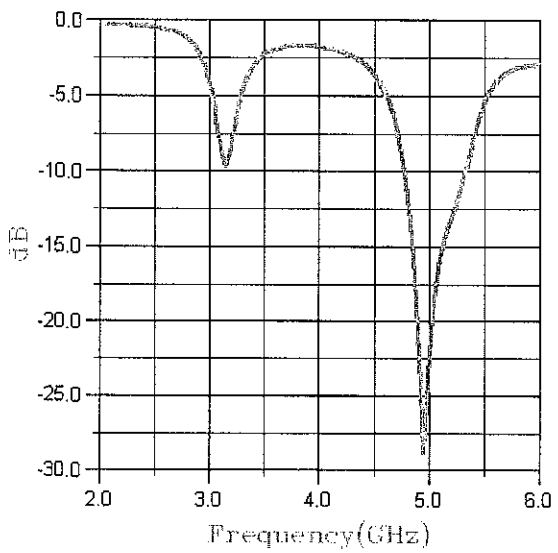

Figure D-8: Position 8

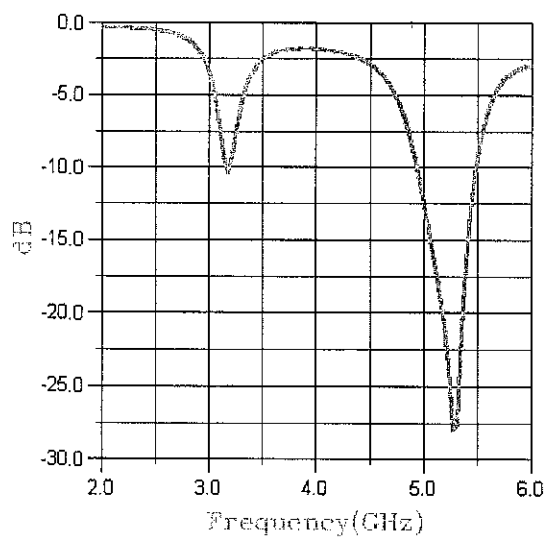

Figure D-9: Position 9

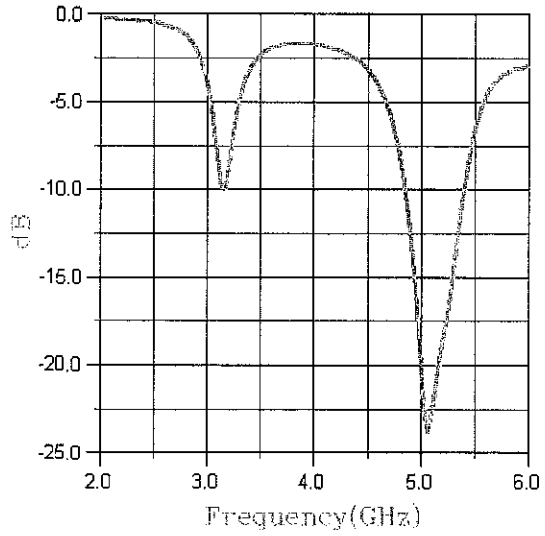

Figure D-10: Position 10

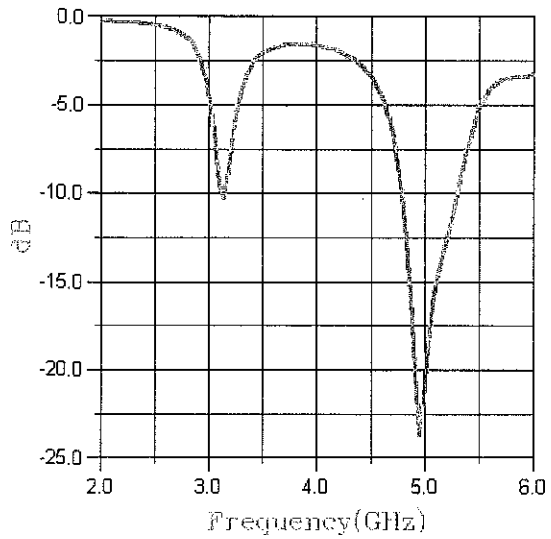

Figure D-11: Position 11

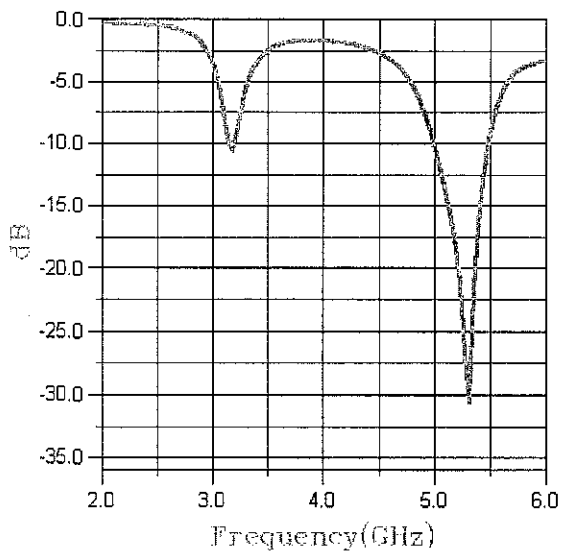

Figure D-12: Position 12

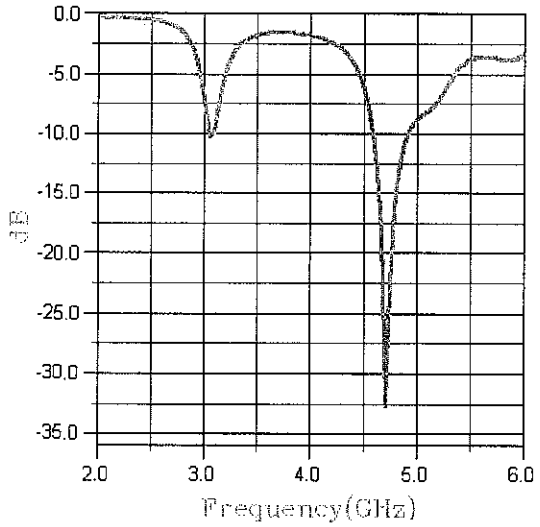

Figure D-13: Position 13

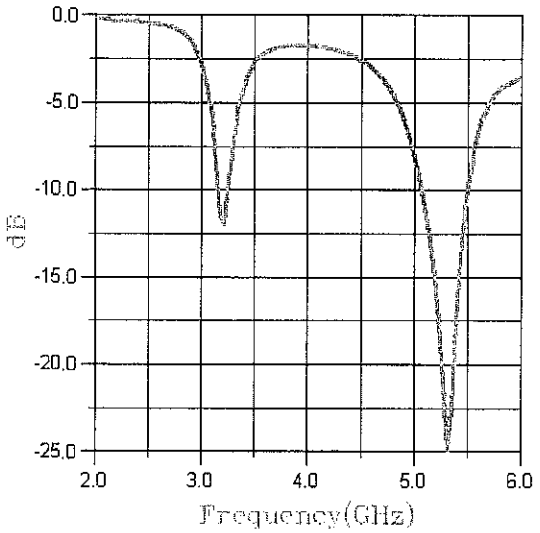

Figure D-14: Position 14

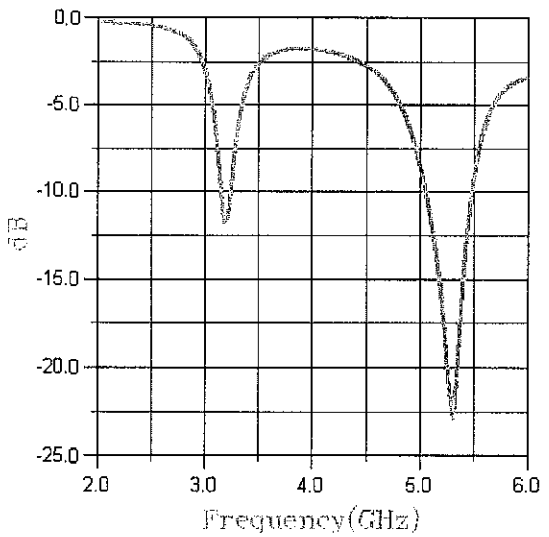

Figure D-15: Position 15

APPENDIX E

S-magnitude plots – Effect of slot size

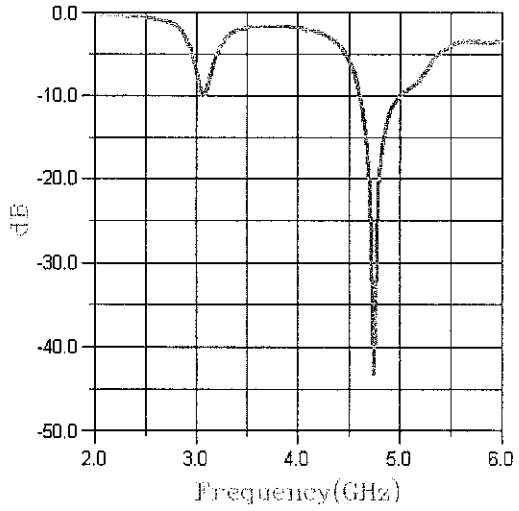

Figure E-1: Slot size 0.2 times the patch size

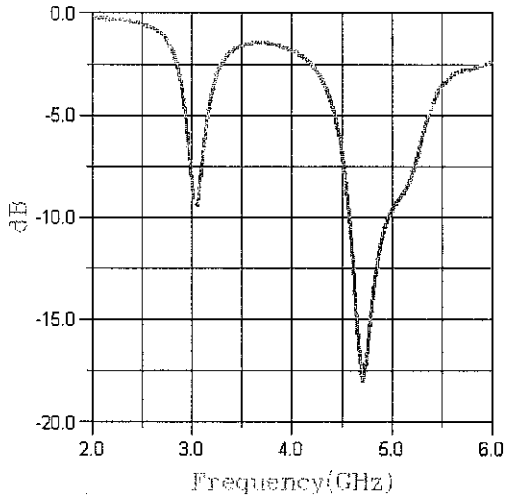

Figure E-2: Slot size 0.3 times the patch size

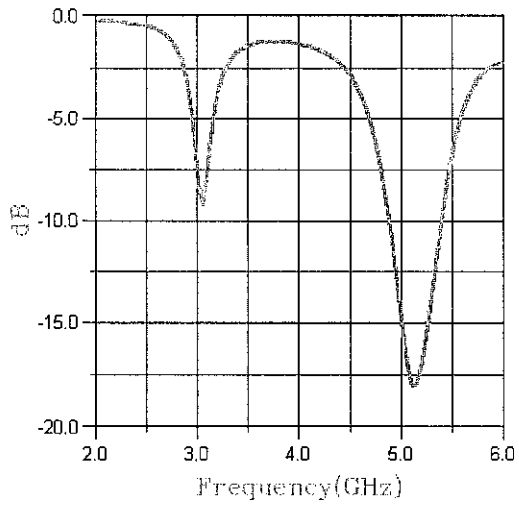

Figure E-3: Slot size 0.4 times the patch size

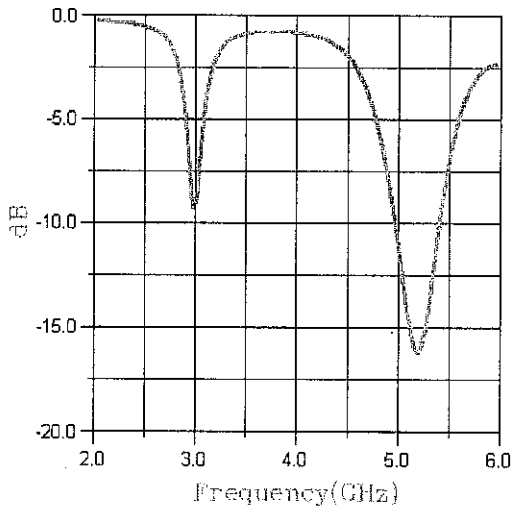

Figure E-4: Slot size 0.5 times the patch size

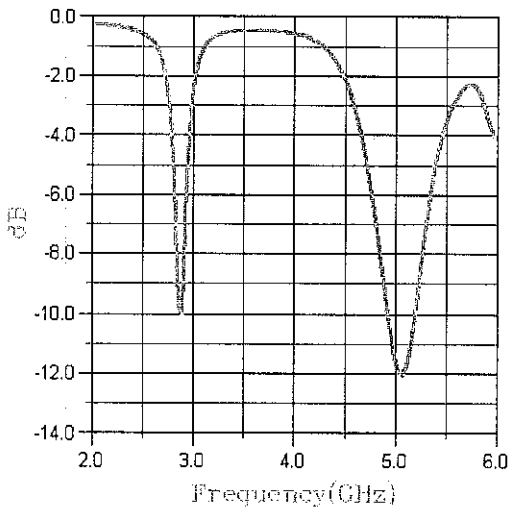

Figure E-5: Slot size 0.6 times the patch size

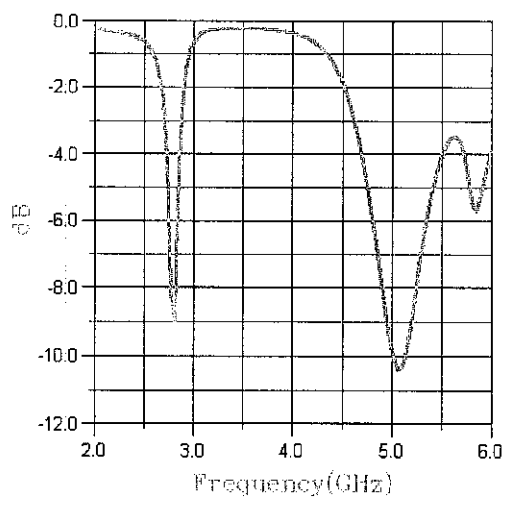

Figure E-6: Slot size 0.7 times the patch size

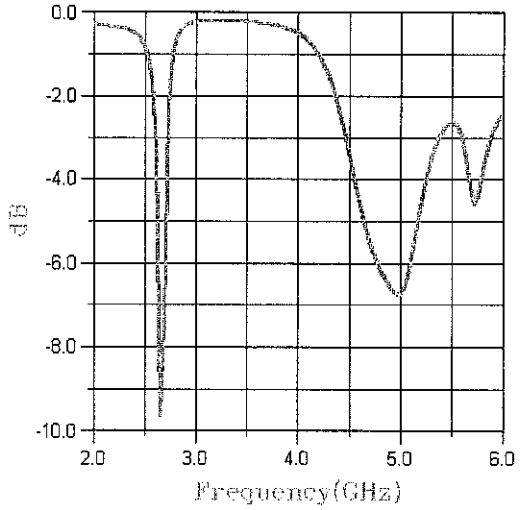

Figure E-7: Slot size 0.8 times the patch size

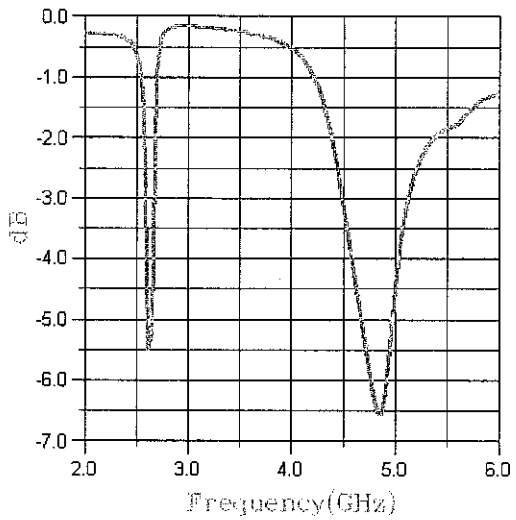

Figure E-8: Slot size 0.9 times the patch size

APPENDIX F

S-magnitude plots – Effect of slot rotation

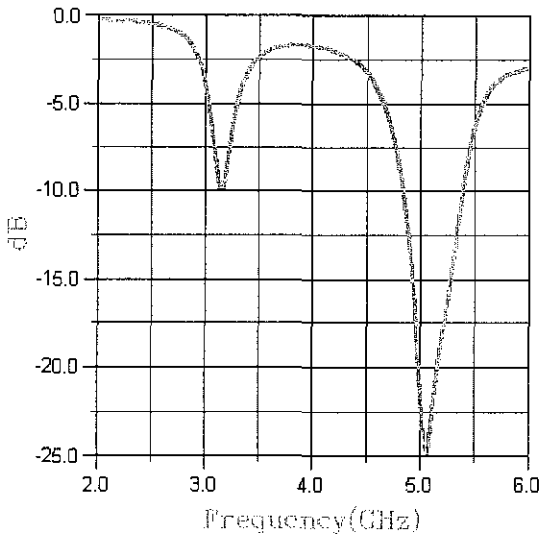

Figure F-1: 20 degree

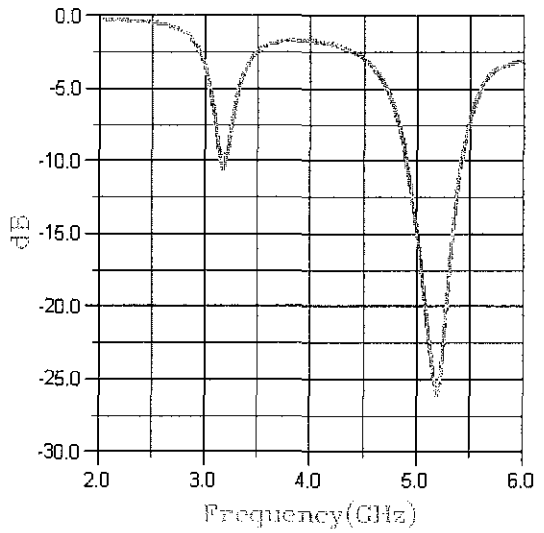

Figure F-2: 30 degree

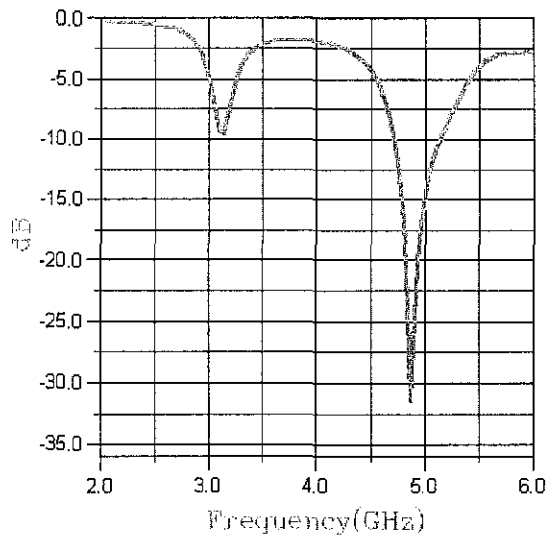

Figure F-3: 40 degree

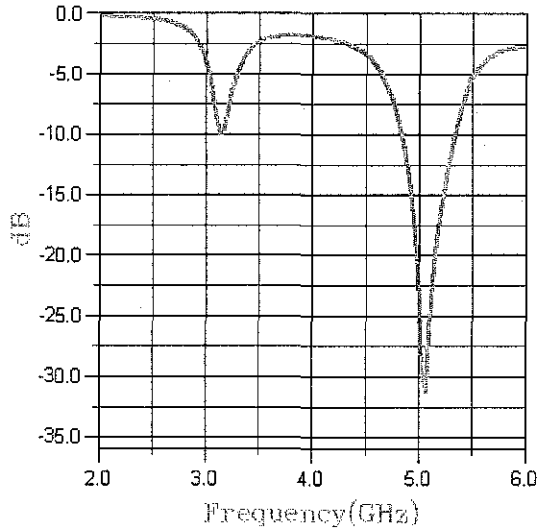

Figure F-4: 45 degree

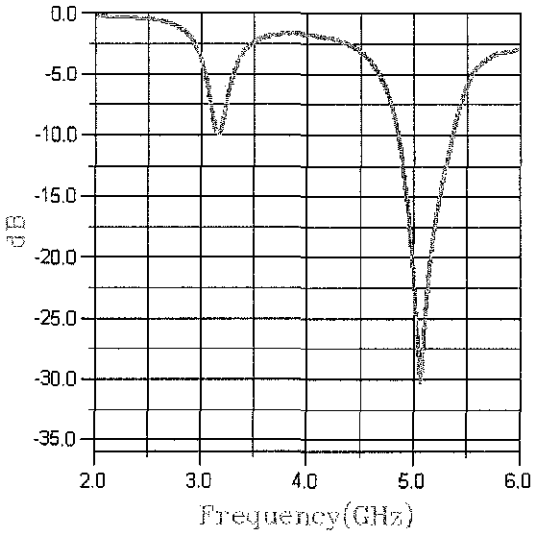

Figure F-5: 60 degree

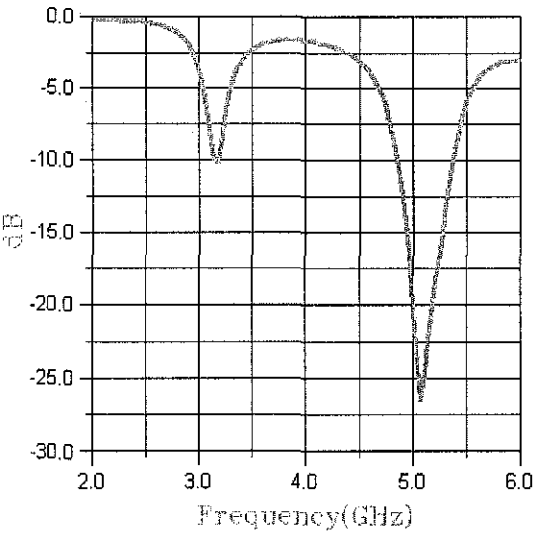

Figure F-6: 90 degree